

Supplementary data

Iridium complexes of acridine-based PNP-type pincer ligands: Synthesis, structure and reactivity

Yarden Lavi,¹ Michael Montag,^{1,*} Yael Diskin-Posner,² Liat Avram,² Linda J. W. Shimon², Yehoshua Ben-David,¹ David Milstein^{1,*}

¹ Department of Molecular Chemistry and Materials Science, Weizmann Institute of Science, Rehovot, Israel

² Department of Chemical Research Support, Weizmann Institute of Science, Rehovot, Israel.

*Corresponding authors: michael.montag@alumni.weizmann.ac.il,
david.milstein@weizmann.ac.il

Table of content

1. NMR spectra	2	
1.1	COMPLEX 1	2
1.2	COMPLEX 2.....	6
1.3	COMPLEX 3	9
1.4	COMPLEX 4.....	12
1.5	COMPLEX 5	15
1.6	COMPLEX 6.....	19
1.7	COMPLEX 7	22
1.8	COMPLEX 9.....	25
1.9	COMPLEX 10.....	29
1.10	COMPLEX 11.....	32
1.11	COMPLEX 12.....	36
1.12	COMPLEX 13.....	40
2. Diffusion-ordered NMR spectroscopy measurements for complexes 3, 6 and 10	43	
3. IR spectra	44	
4. GC-TCD measurement for gas phase in the formation of complexes 5 AND 6	45	
5. X-ray data collection and structure refinement	46	
6. Crystal structure of complex 8	48	
7. ICP-OES measurements associated with complexes 5 and 9	49	
8. References	50	

1. NMR spectra

1.1 Complex 1

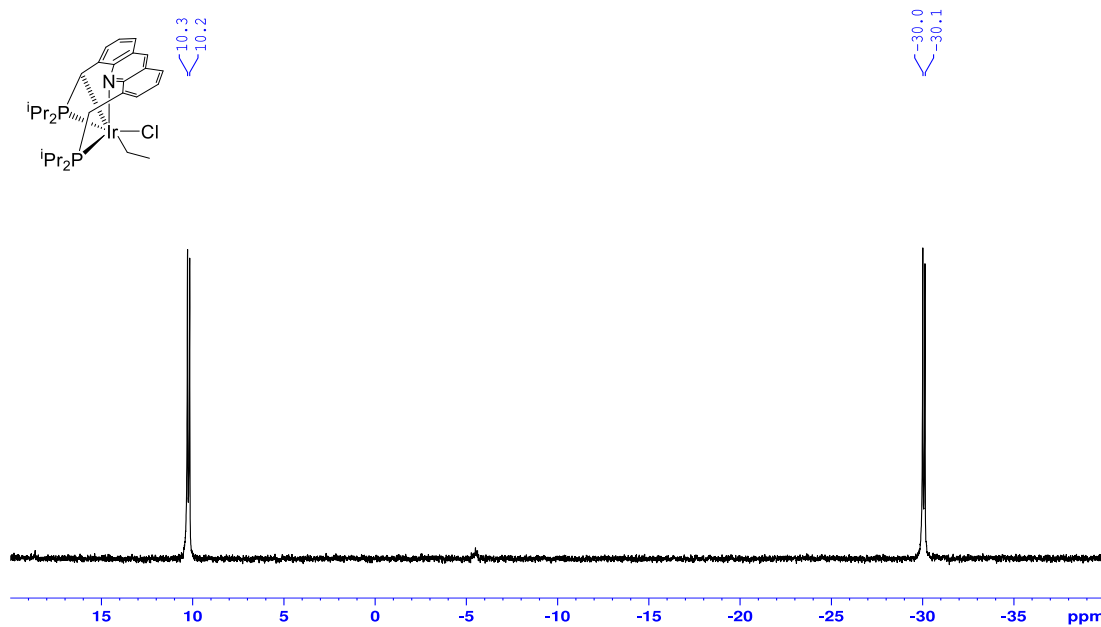


Figure S1. Complex 1 – $^{31}\text{P}\{\text{H}\}$ NMR spectrum in THF- d_8 .

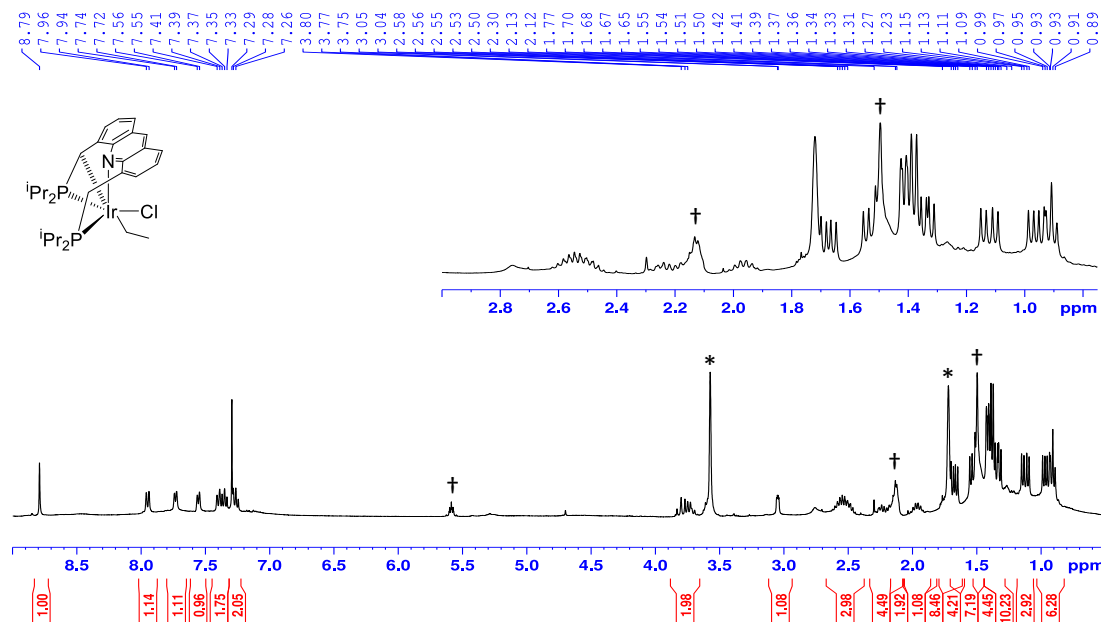


Figure S2. Complex 1 – ^1H NMR spectrum in THF- d_8 . * = residual solvent peak. † = residual cyclooctene.

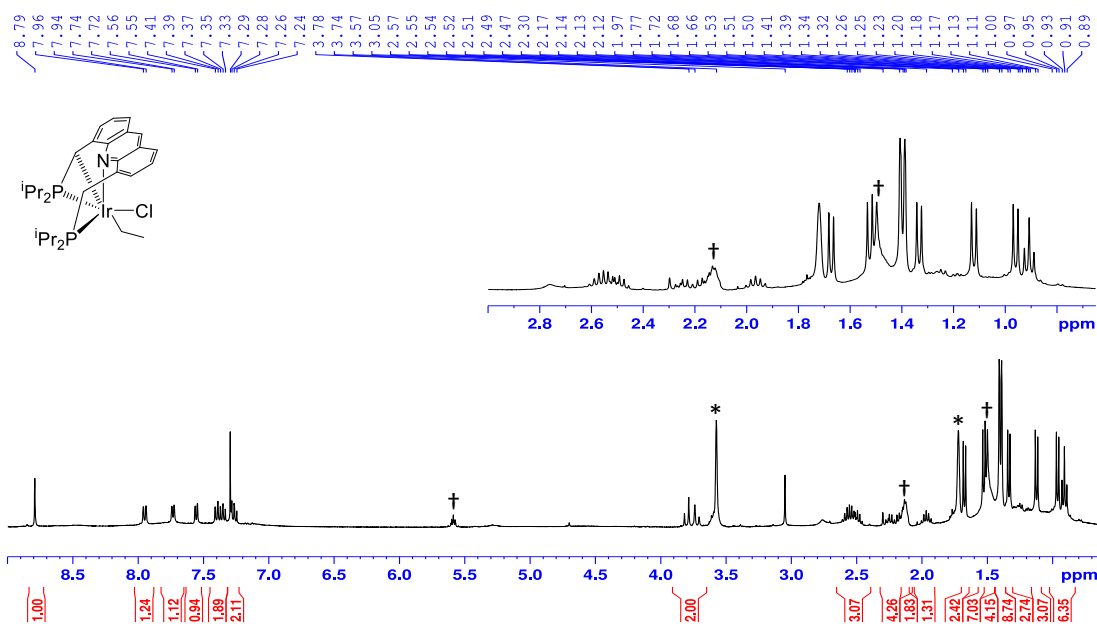


Figure S3. Complex **1** – $^1\text{H}\{^{31}\text{P}\}$ NMR spectrum in THF-d₈. * = residual solvent peak. † = residual cyclooctene.

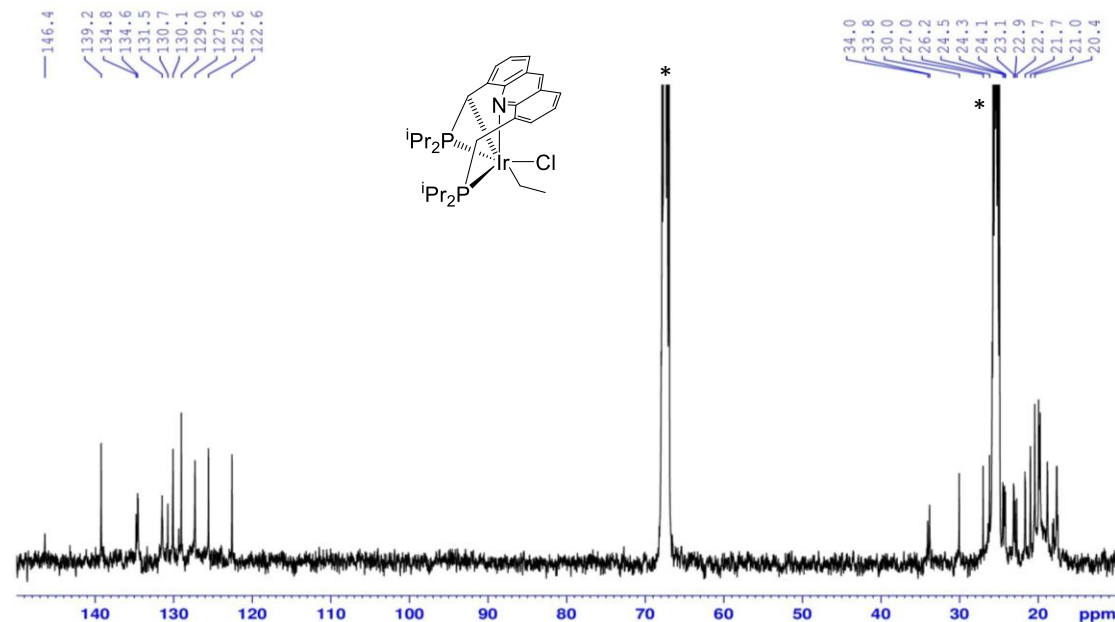


Figure S4. Complex **1** – $^{13}\text{C}\{\text{H}\}$ NMR in THF-d₈. * = residual solvent peak.

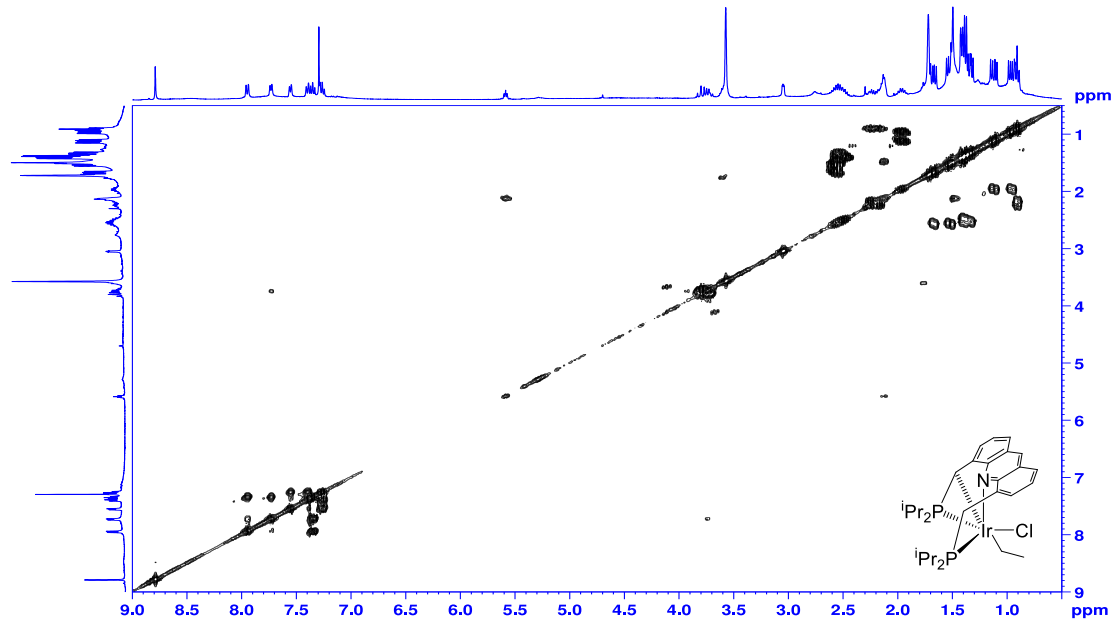


Figure S5. Complex **1** – ^1H COSY spectrum in $\text{THF}-\text{d}_8$.

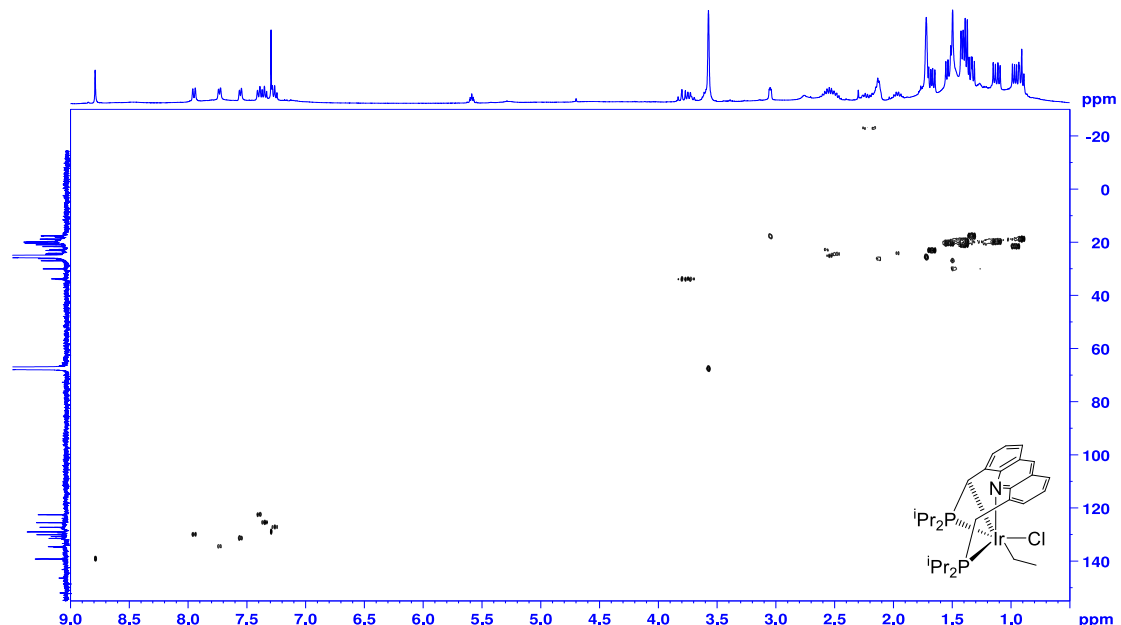


Figure S6. Complex **1** – ^{13}C - ^1H HSQC spectrum in $\text{THF}-\text{d}_8$.

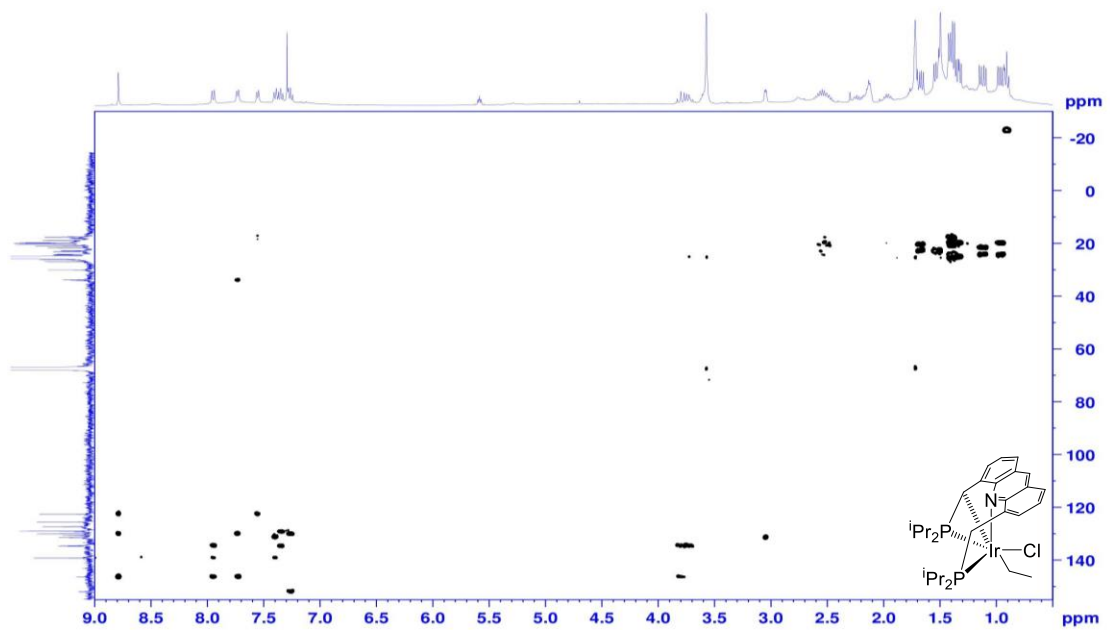


Figure S7. Complex **1** – ^{13}C - ^1H HMBC spectrum in THF-d_8 .

1.2 Complex 2

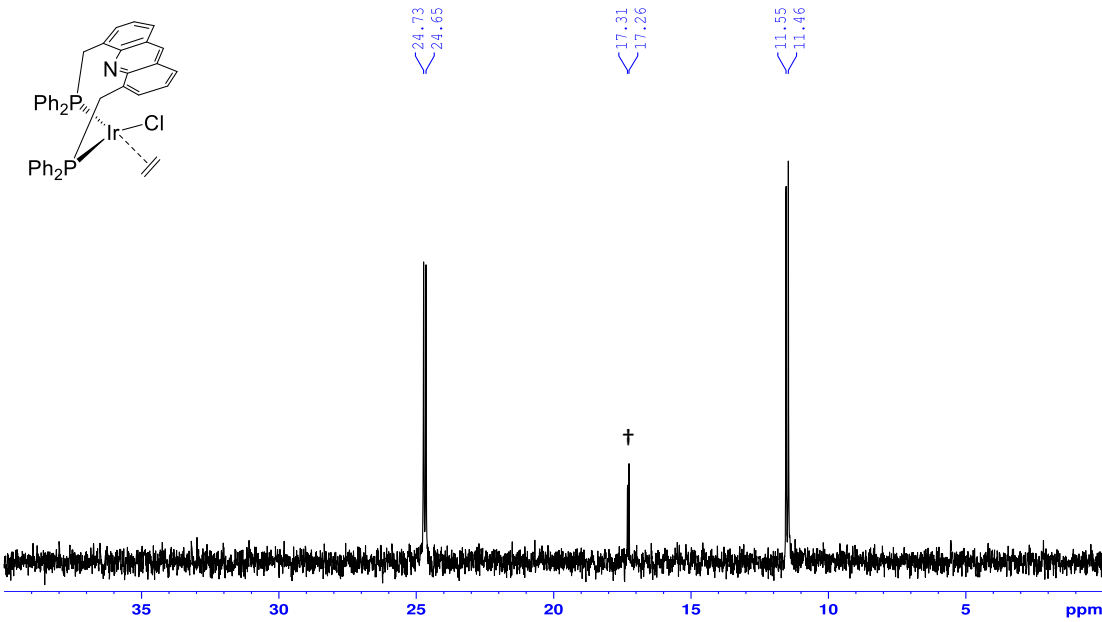


Figure S8. Complex **2** – $^{31}\text{P}\{\text{H}\}$ NMR spectrum in CD_2Cl_2 at -20 °C. Complex **2** is unstable in solution and an impurity is formed (\dagger).

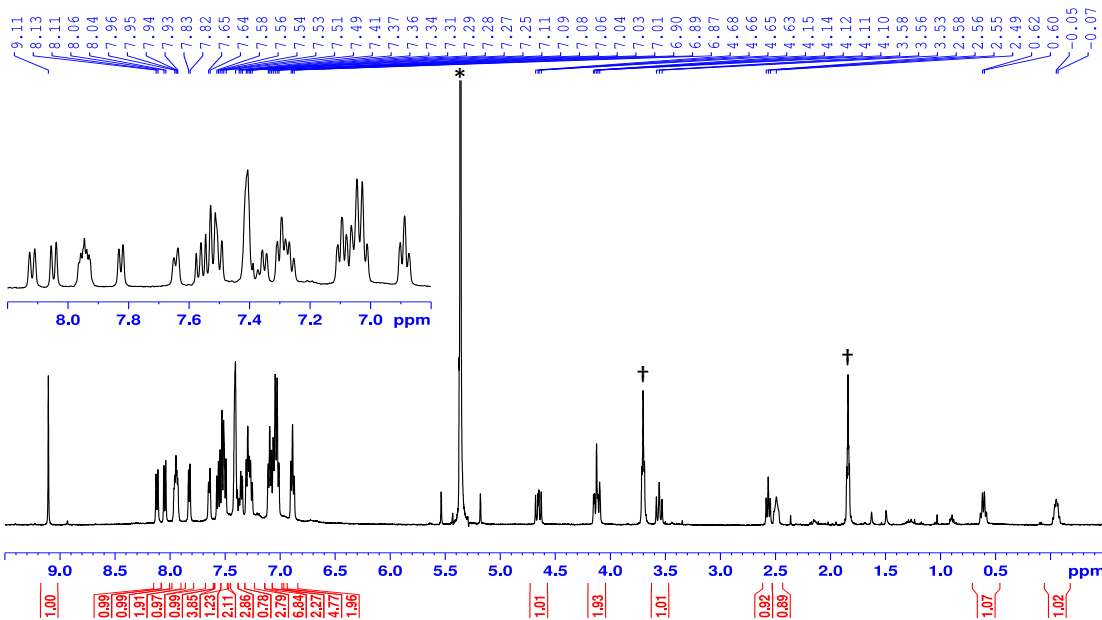


Figure S9. Complex **2** – ^1H NMR spectrum in CD_2Cl_2 at -20°C . * = residual solvent peak. † = residual THF.

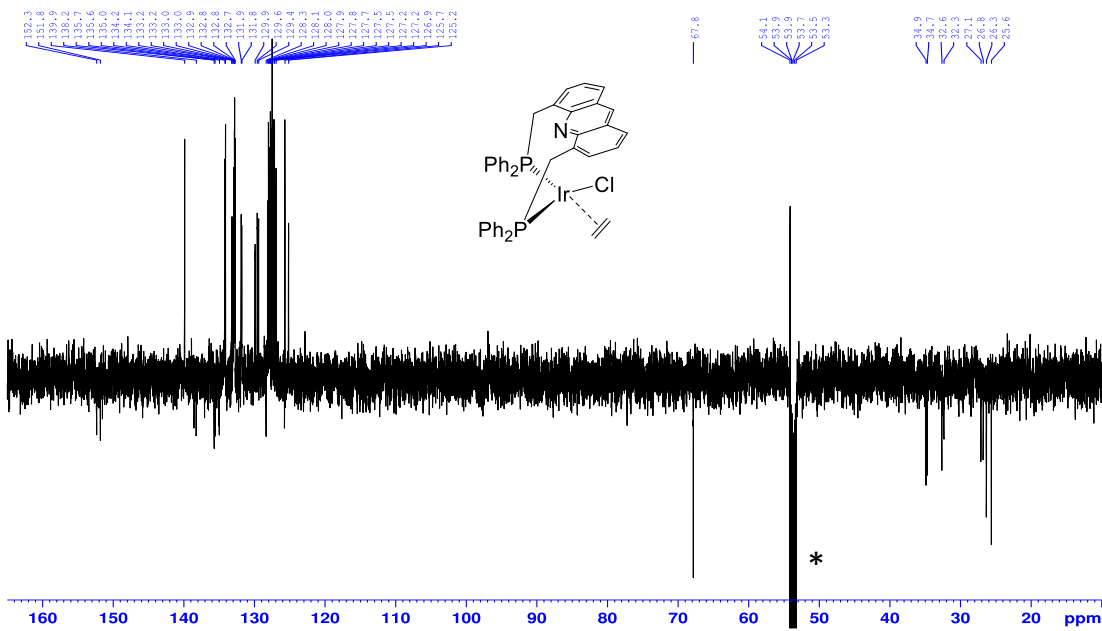


Figure S10. Complex **2** – ^{13}C DEPTQ spectrum in CD_2Cl_2 at -20 °C. * = residual solvent peak.

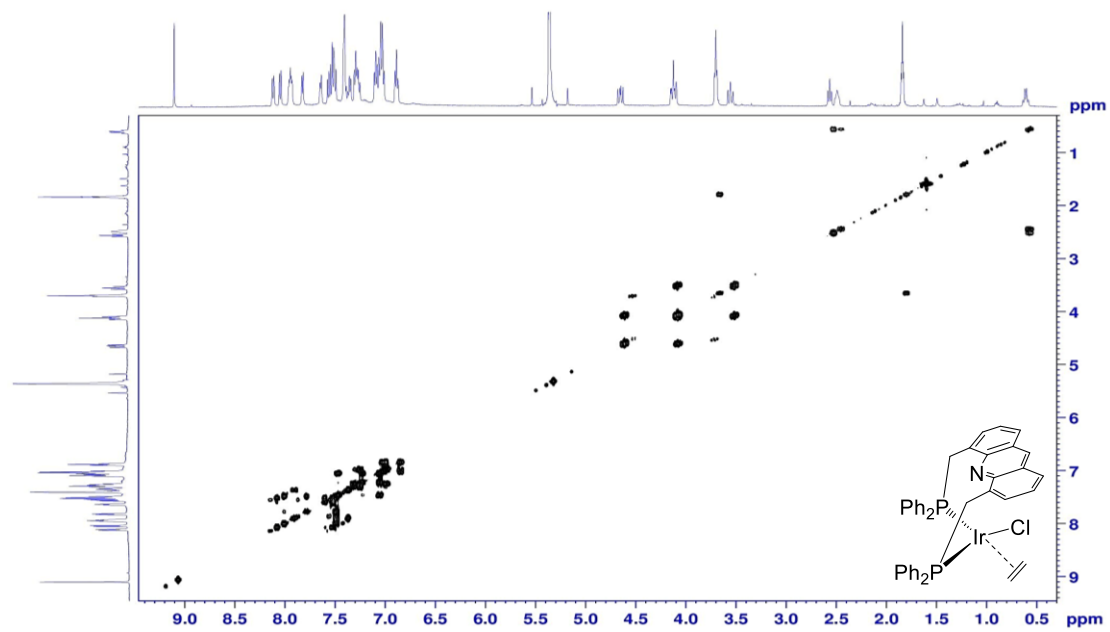


Figure S11. Complex 2 – ^1H COSY spectrum in CD_2Cl_2 at -20 °C.

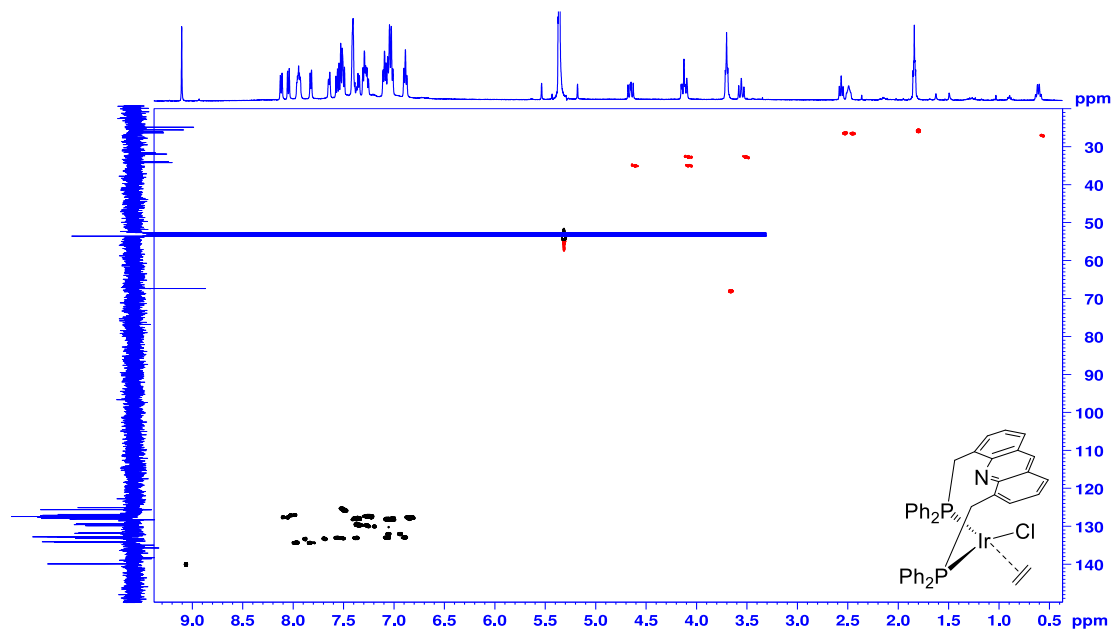


Figure S12. Complex 2 – ^{13}C - ^1H HSQC spectrum in CD_2Cl_2 at -20°C .

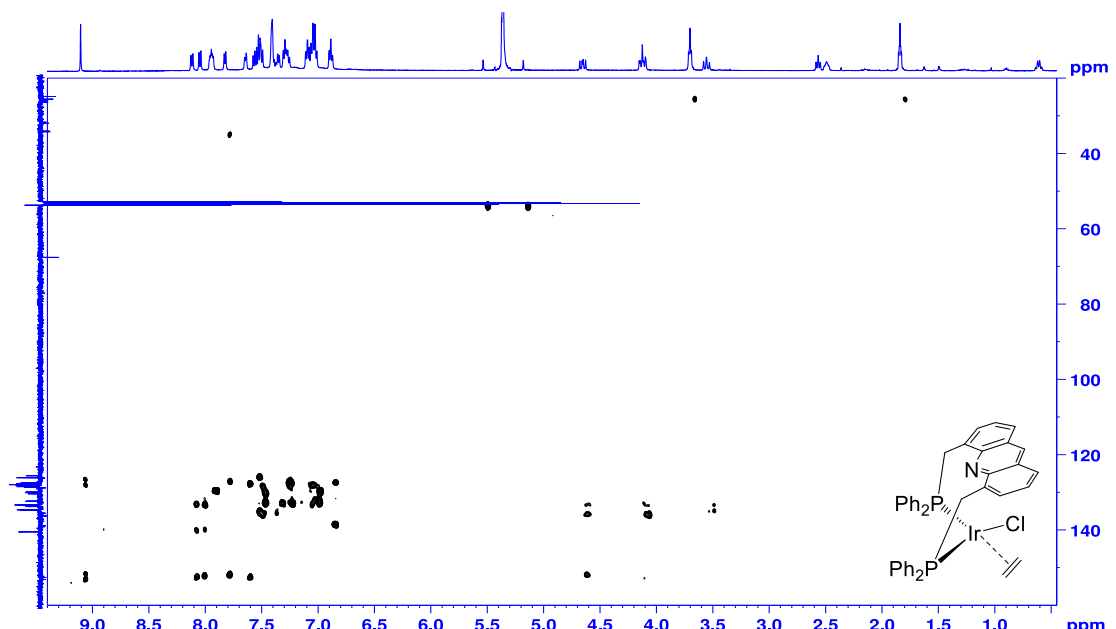


Figure S13. Complex 2 – ^{13}C - ^1H HMBC spectrum in CD_2Cl_2 at -20°C .

1.3 complex 3

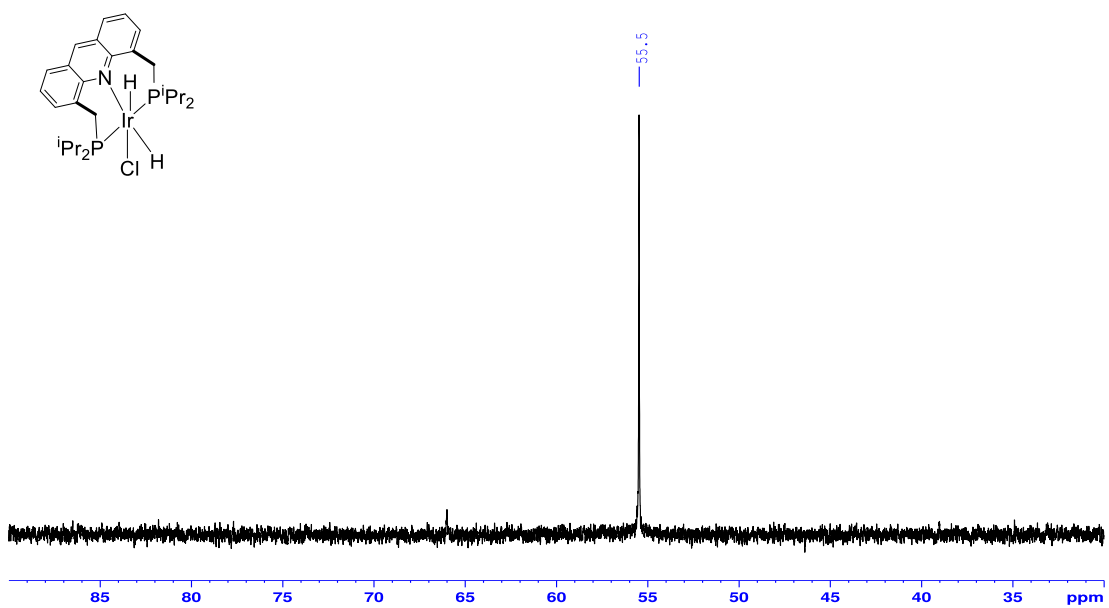


Figure S14. Complex 3 – $^{31}\text{P}\{\text{H}\}$ NMR spectrum in C_6D_6 .

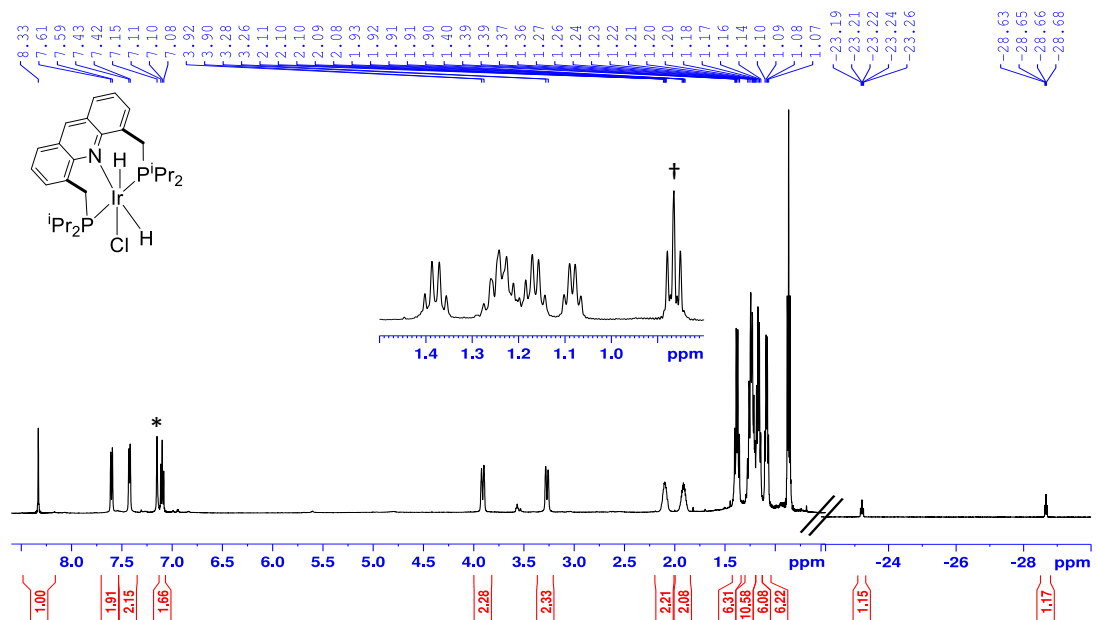


Figure S15. Complex 3 – ^1H NMR spectrum in C_6D_6 . * = residual solvent peak. † = residual pentane.

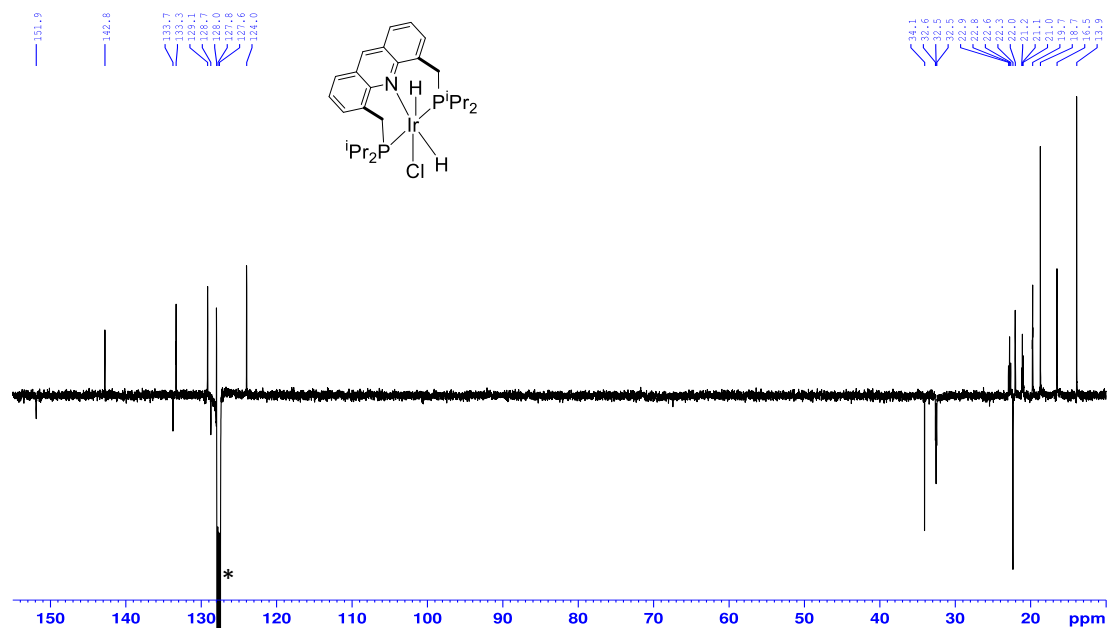


Figure S16. Complex 3 – ^{13}C DEPTQ spectrum in C_6D_6 . * = residual solvent peak.

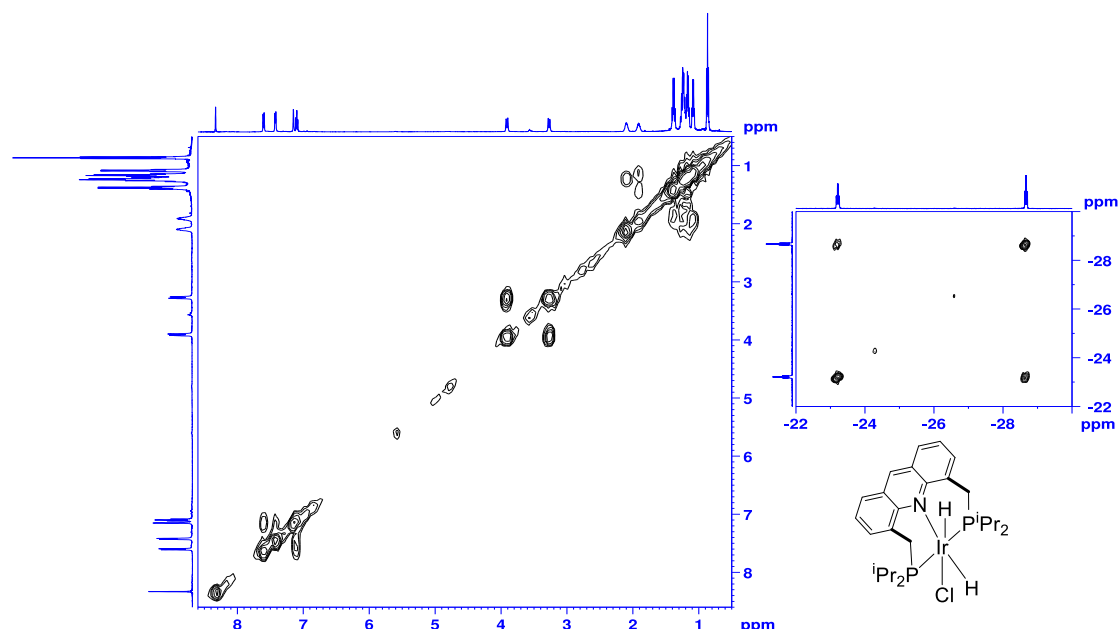


Figure S17. Complex 3 – ^1H COSY spectrum in C_6D_6 . Left image: 0 to 9 ppm. Right image: -30 to -22 ppm.

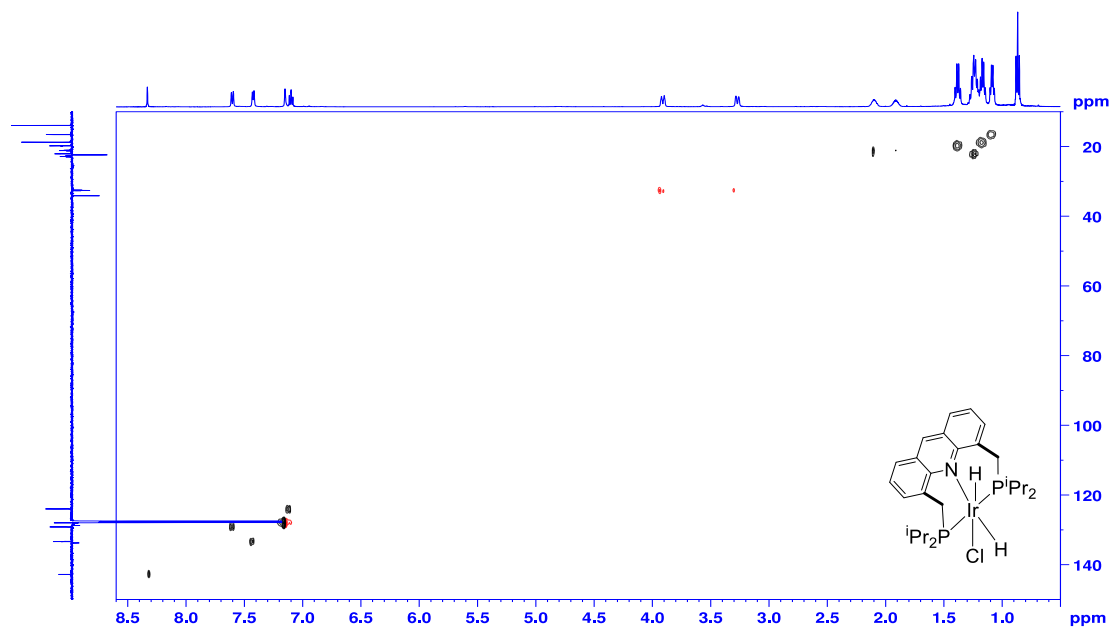


Figure S18. Complex **3** – ^{13}C - ^1H HSQC spectrum in C_6D_6 .

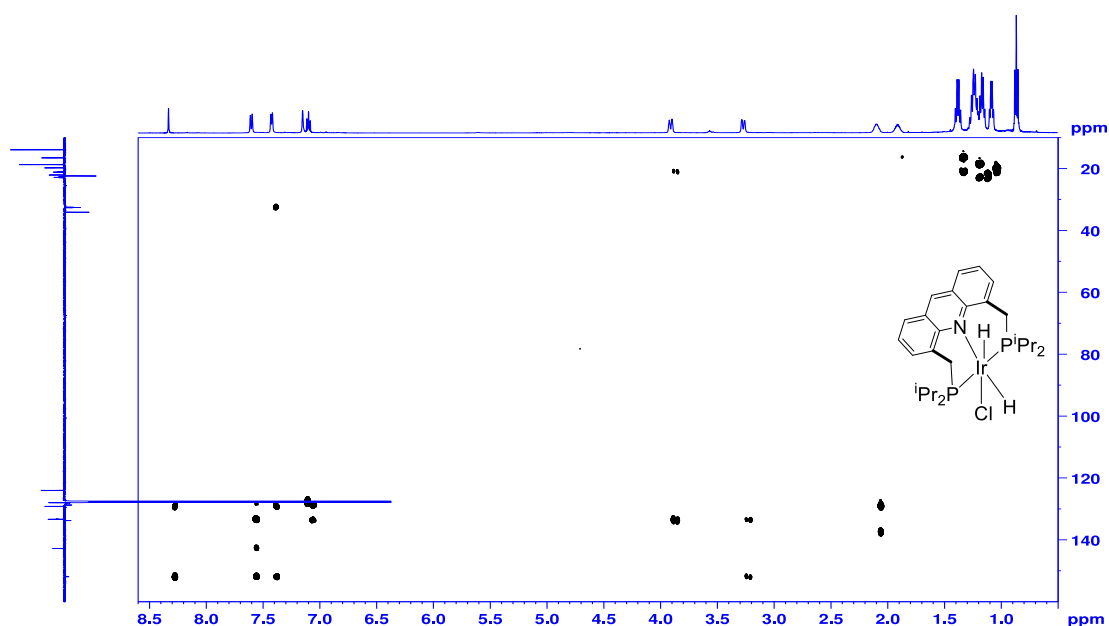


Figure S19. Complex **3** – ^{13}C - ^1H HMBC spectrum in C_6D_6 .

1.4 Complex 4

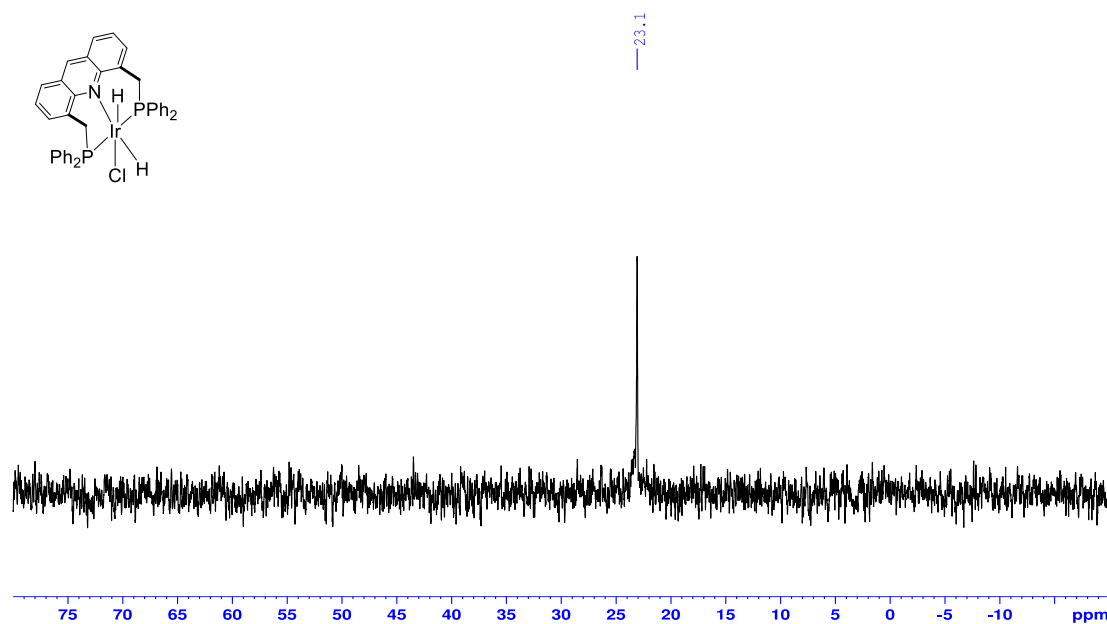


Figure S20. Complex 4. ³¹P{¹H} NMR spectrum in CDCl₃.

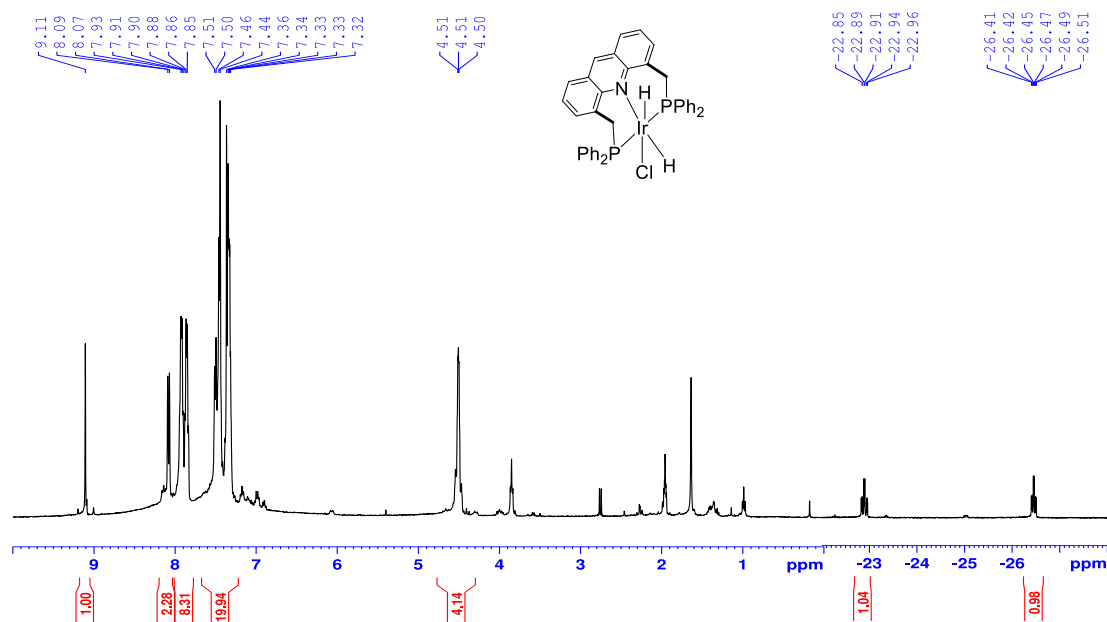


Figure S21. Complex 4 – ¹H NMR spectrum in CDCl₃. The peaks in the range 0–4 ppm belong to residual THF, pentane and water.

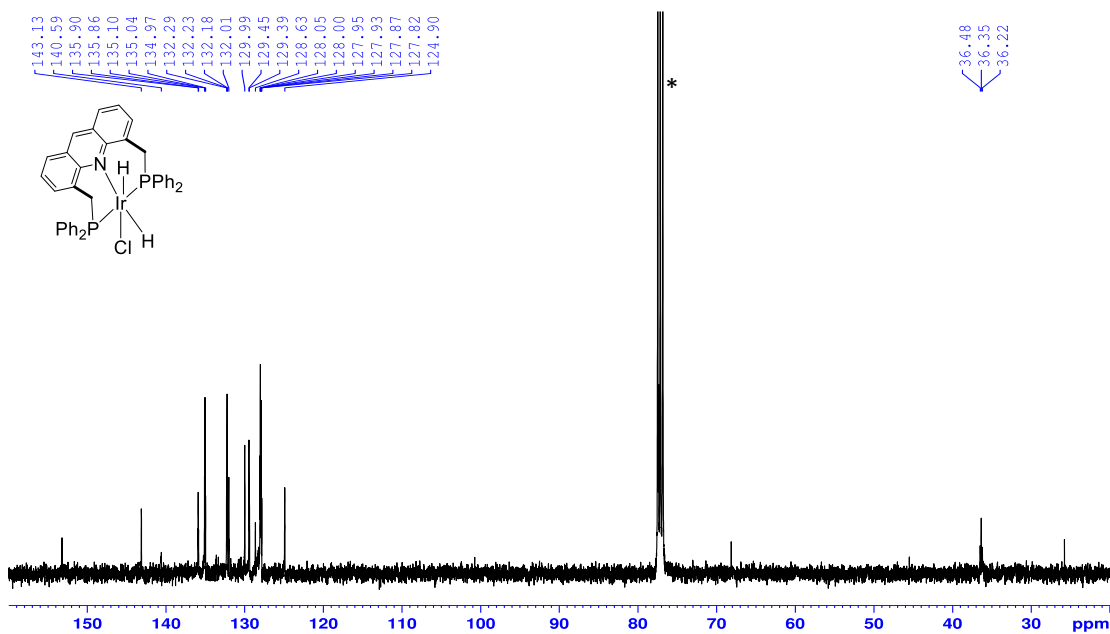


Figure S22. Complex 4 – $^{13}\text{C}\{^1\text{H}\}$ NMR spectrum in CDCl_3 . * = residual solvent peak.

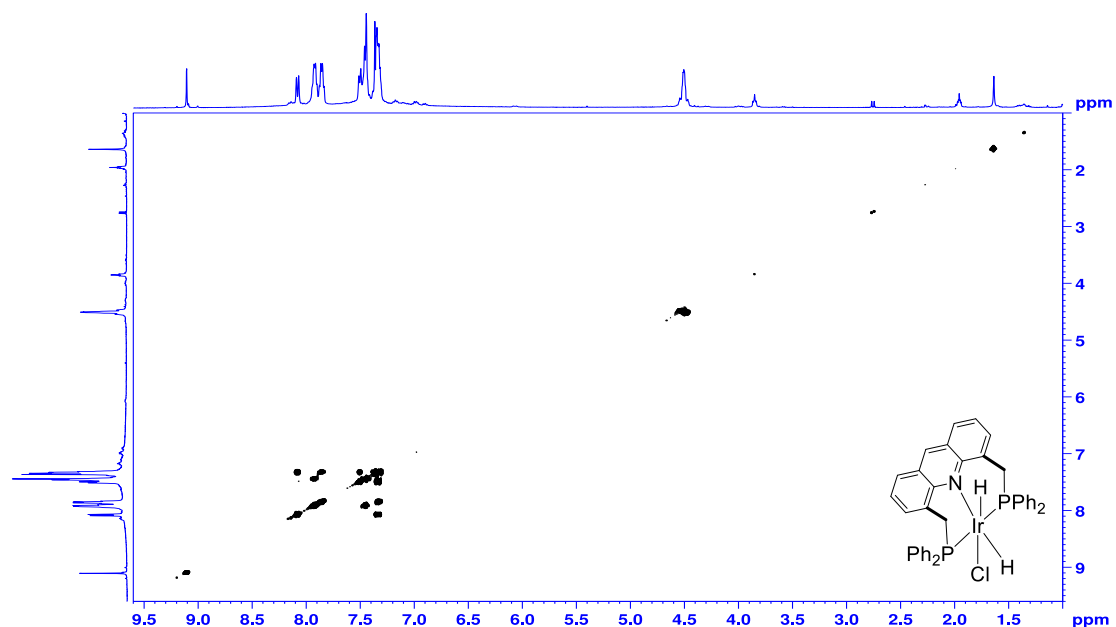


Figure S23. Complex 4 – ^1H COSY spectrum in CDCl_3 .

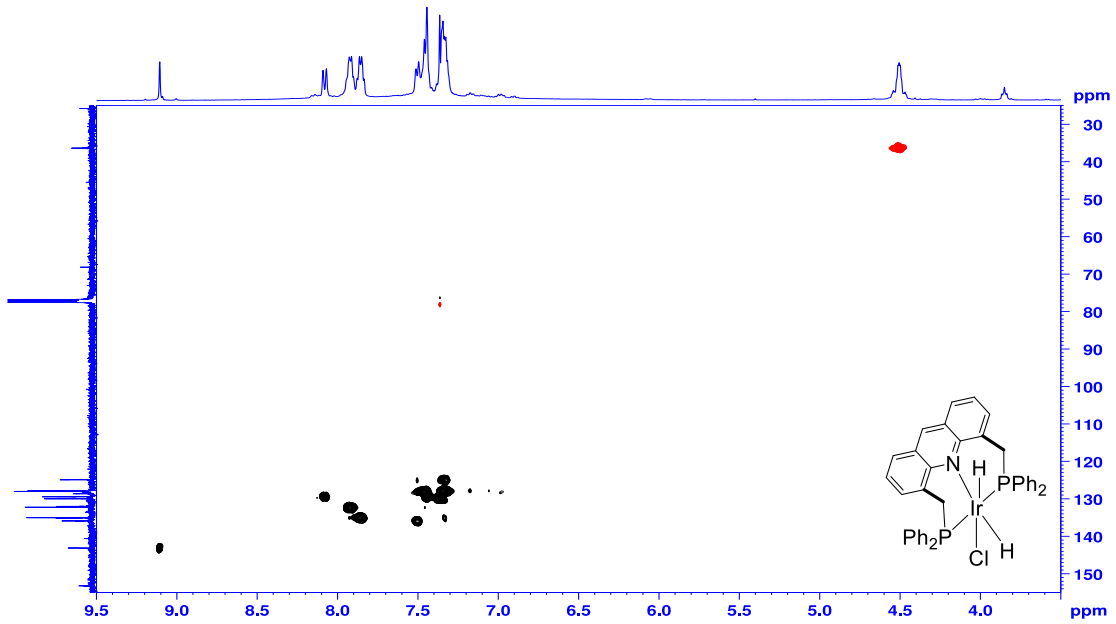


Figure S24. Complex 4 – ^{13}C - ^1H HSQC spectrum in CDCl_3 .

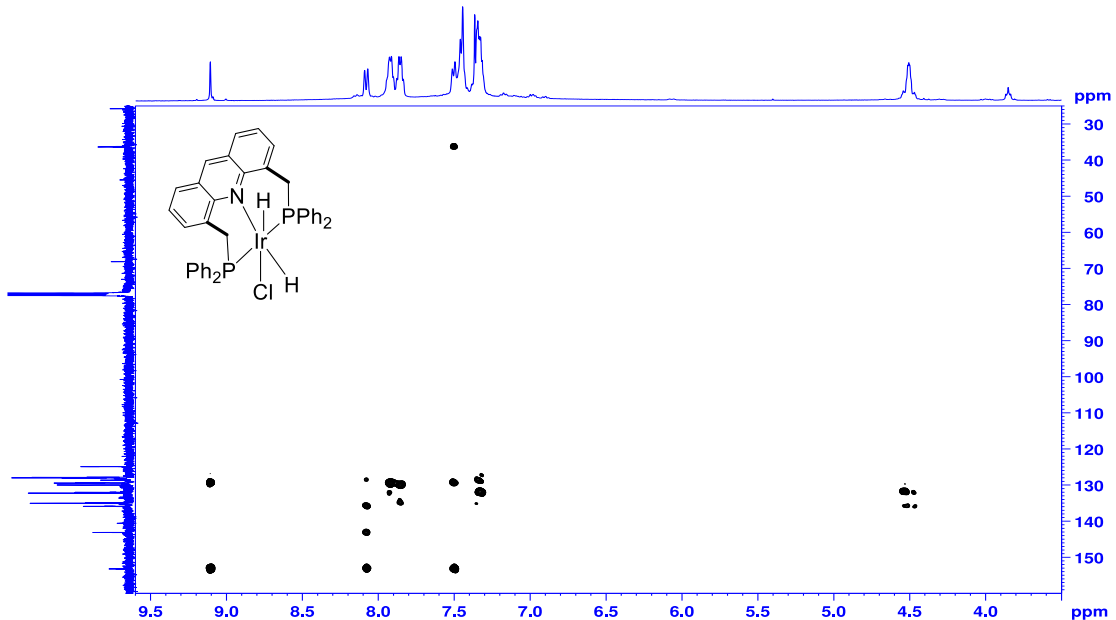


Figure S25. Complex 4 – ^{13}C - ^1H HMBC spectrum in CDCl_3 .

1.5 complex 5

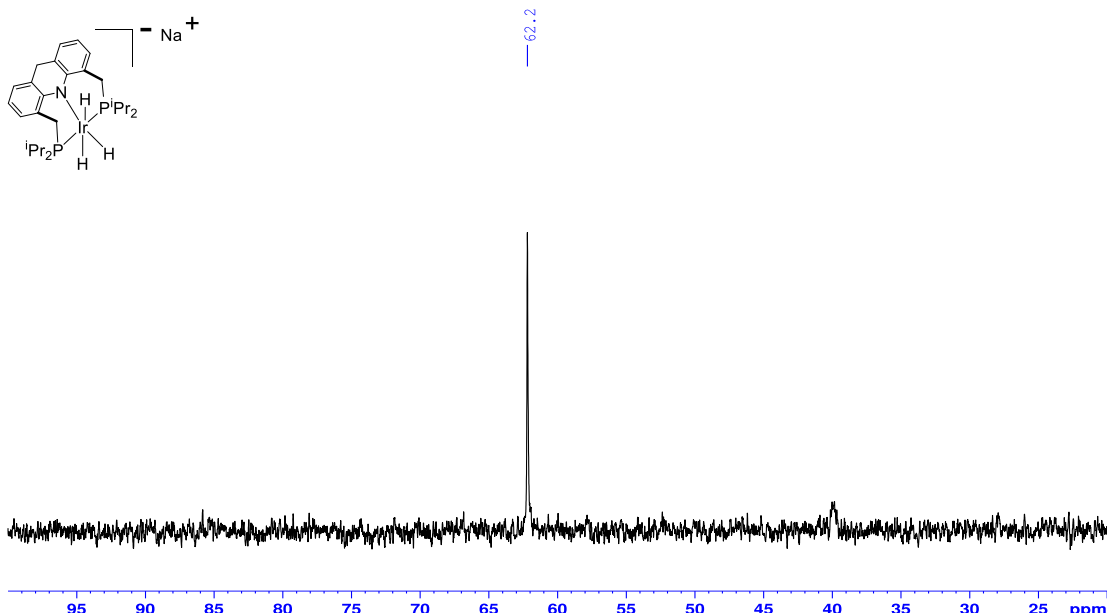


Figure S26. Complex 5 – ³¹P{¹H} NMR spectrum in THF-d₈ at -20 °C (complex was generated *in situ*).

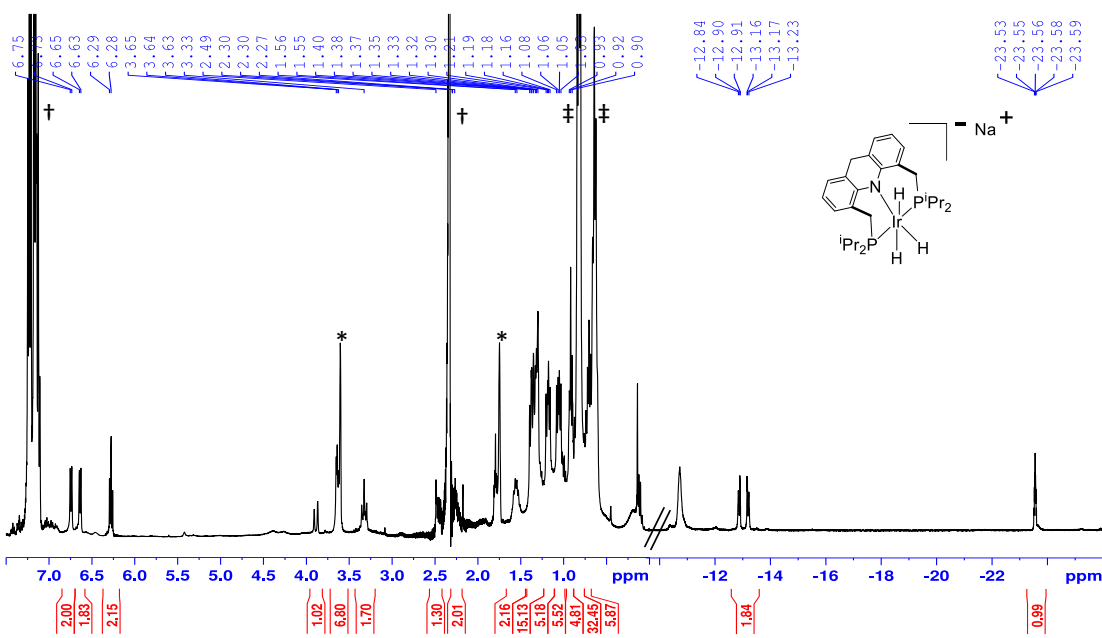


Figure S27. Complex 5 – ¹H NMR spectrum in THF-d₈ at -20 °C (complex was generated *in situ*). * = residual solvent peak. † = toluene from the NaBET₃H solution. ‡ = BET₃ byproduct.

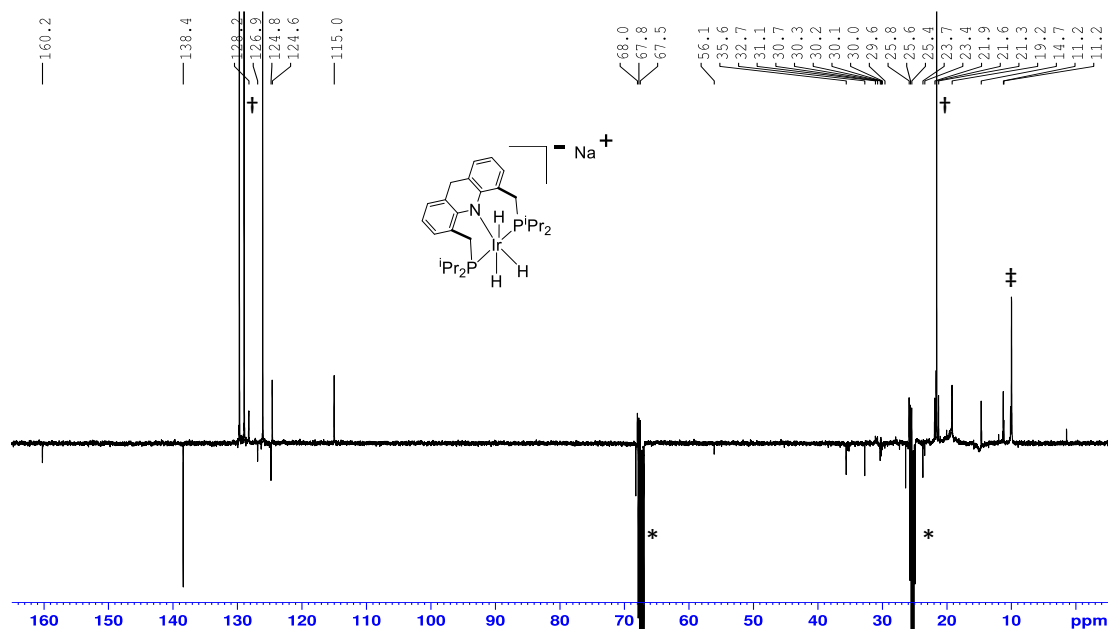


Figure S28. Complex **5** – ^{13}C DEPTQ spectrum in THF-d_8 at $-20\text{ }^\circ\text{C}$ (complex was generated *in situ*). * = residual solvent peak. † = toluene from the NaBET_3H solution. ‡ = BEt_3 byproduct.

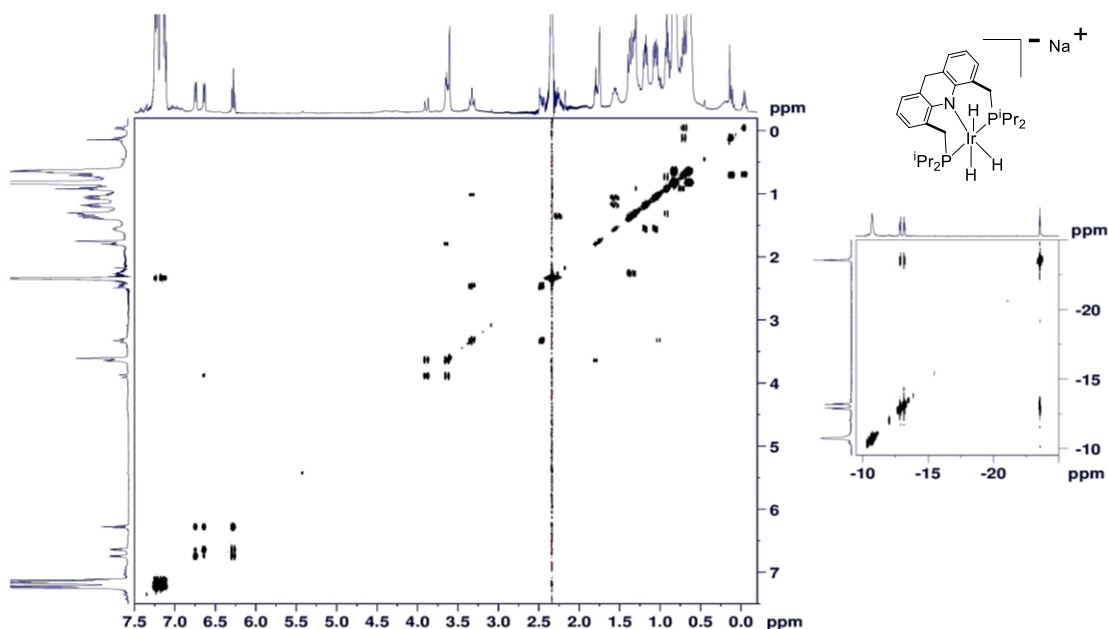


Figure S29. Complex **5** – ^1H COSY spectrum in THF-d_8 at $-20\text{ }^\circ\text{C}$ (complex was generated *in situ*). Left image: 0.0 to 7.5 ppm. Right image: -25 to -10 ppm.

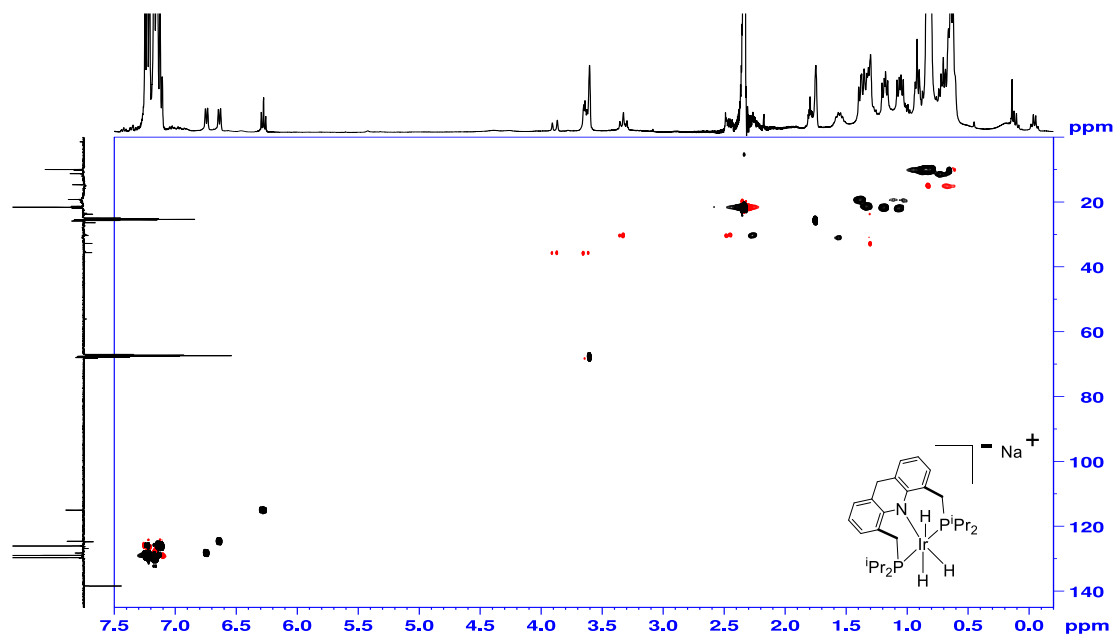


Figure S30. Complex 5 – ^{13}C - ^1H HSQC spectrum in THF-d_8 at -20°C (complex was generated *in situ*).

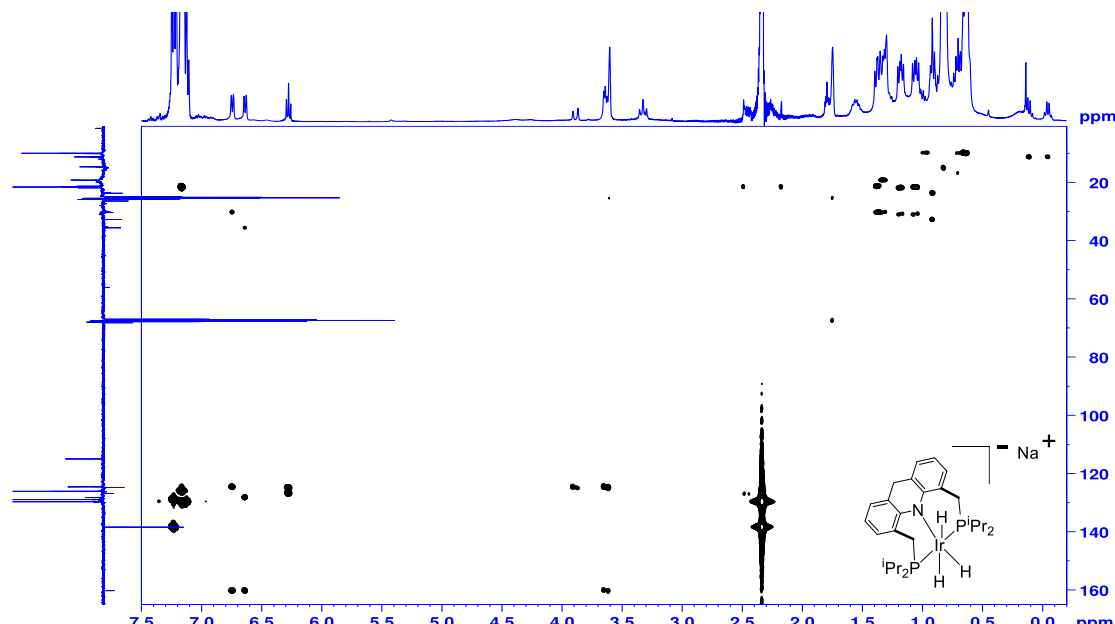


Figure S31. Complex 5 – ^{13}C - ^1H HMBC spectrum in THF-d_8 at -20°C (complex was generated *in situ*).

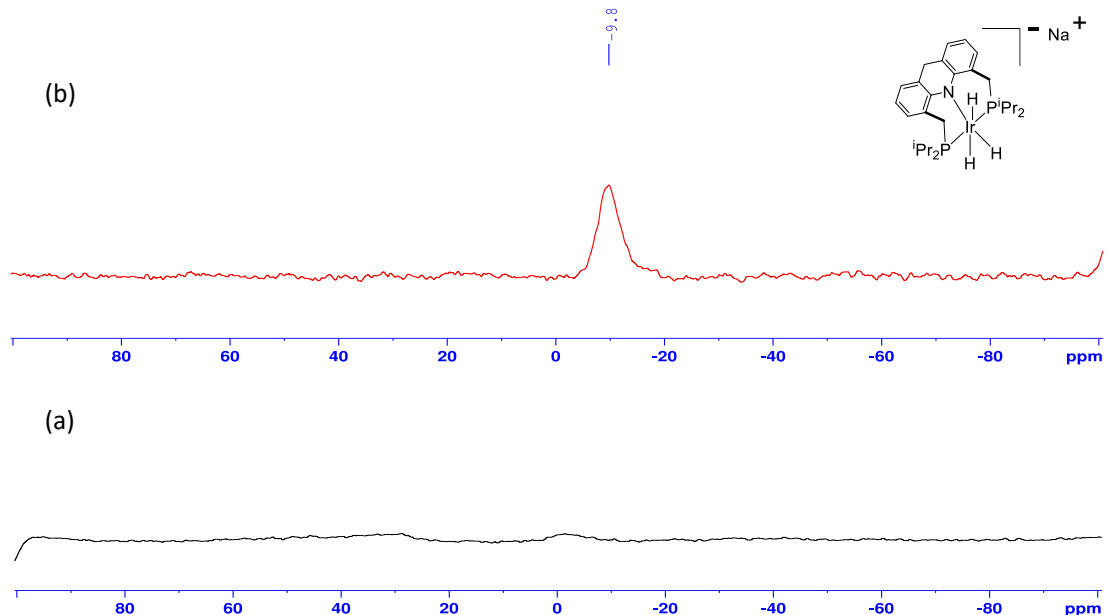


Figure S32. Complex **5** – ^{23}Na NMR spectra in THF at room temperature (complex was generated *in situ*). (a) 5 minutes after generation of the complex. (b) After addition of 2 equiv of 18-crown-6.

1.6 complex 6

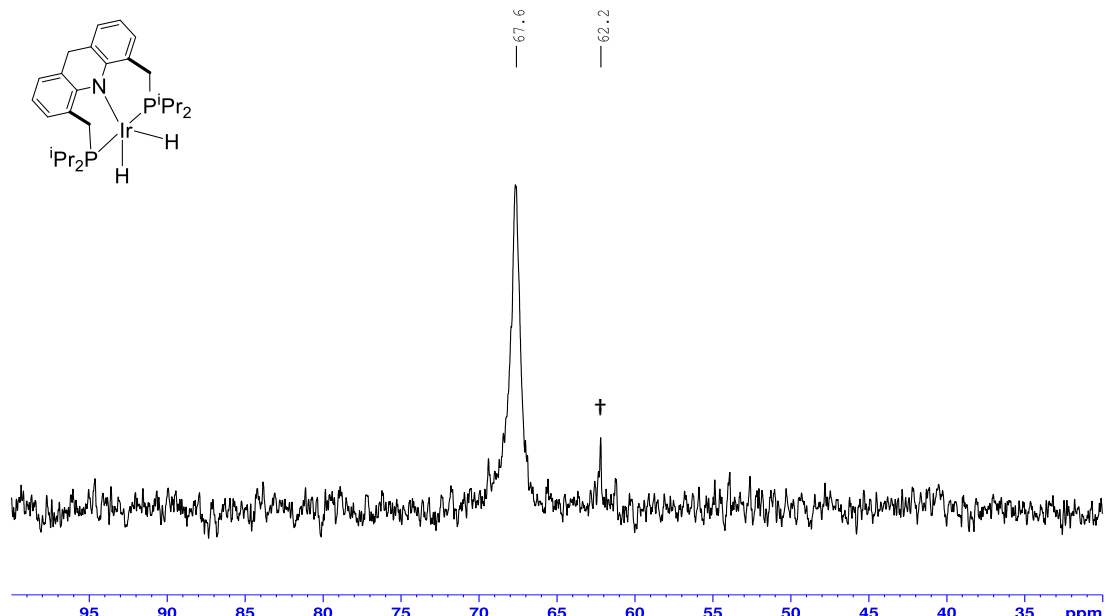


Figure S33. Complex 6 – $^{31}\text{P}\{\text{H}\}$ NMR spectrum in THF- d_8 at -30°C . † = residual complex 5 .

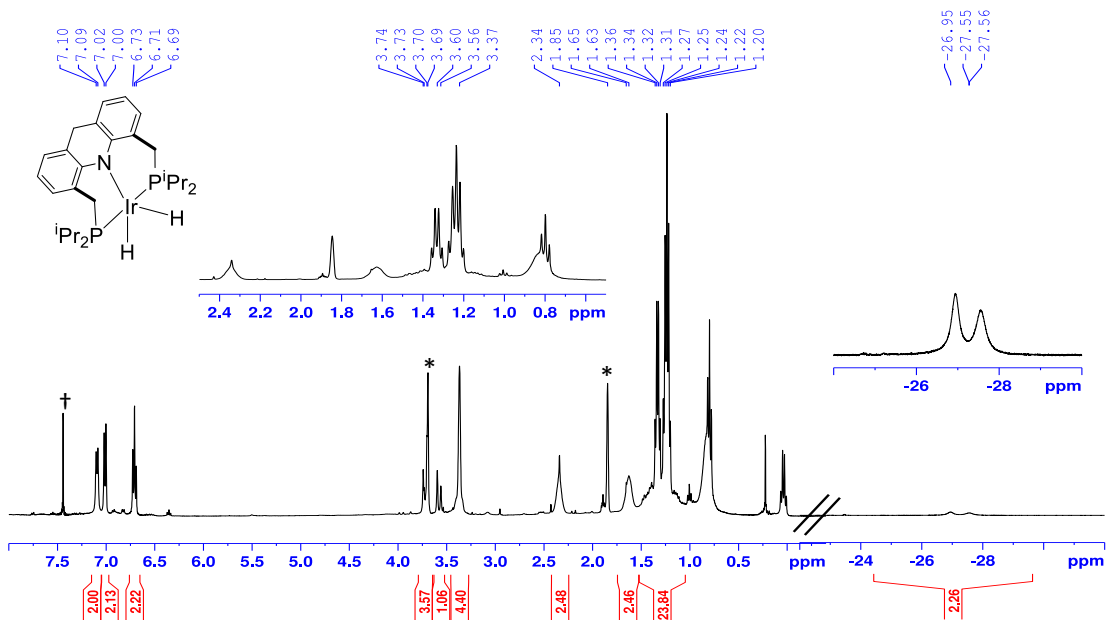


Figure S34. Complex 6 – ^1H NMR spectrum in THF- d_8 at -30°C . * = residual solvent peak. † = residual benzene.

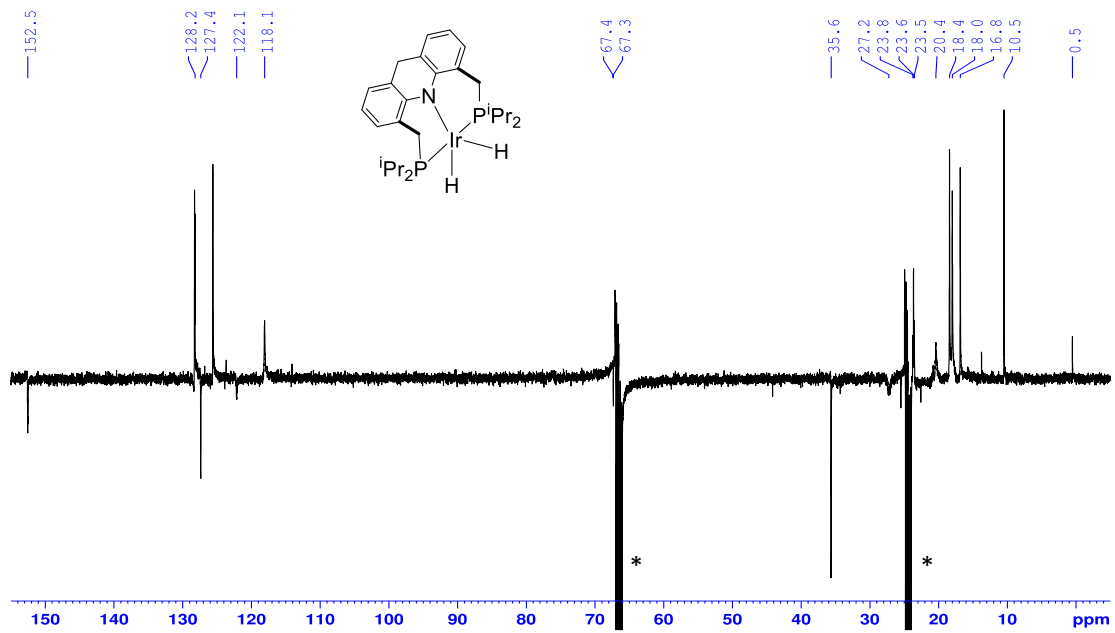


Figure S35. Complex **6** – ^{13}C DEPTQ spectrum in THF-d_8 at $-30\text{ }^\circ\text{C}$. * = residual solvent peak.

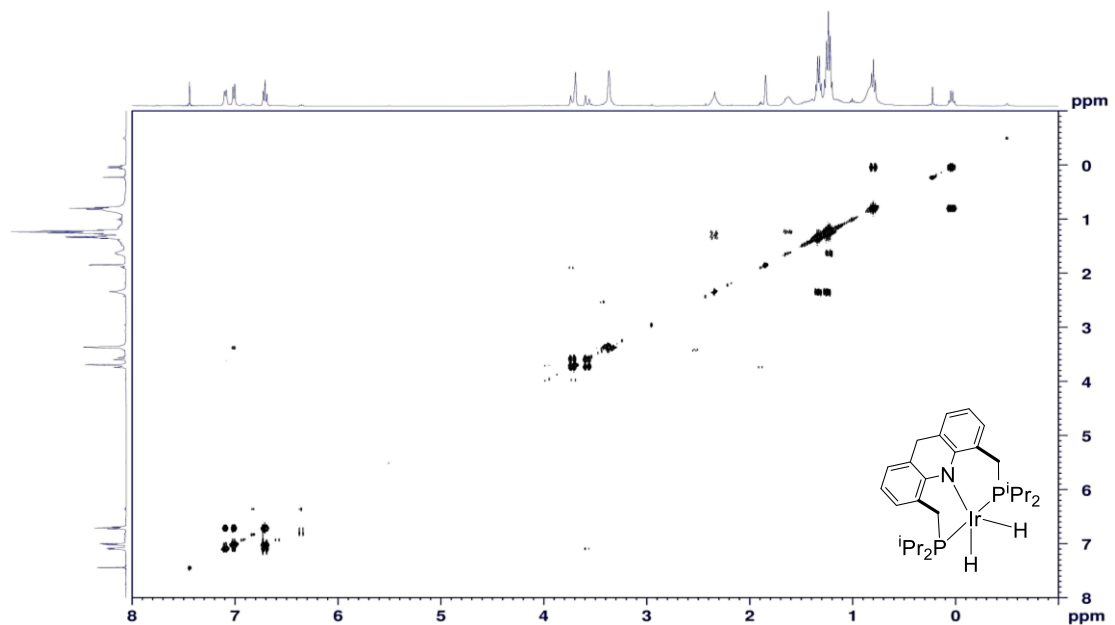


Figure S36. Complex **6** – ^1H COSY spectrum in THF-d_8 at $-30\text{ }^\circ\text{C}$.

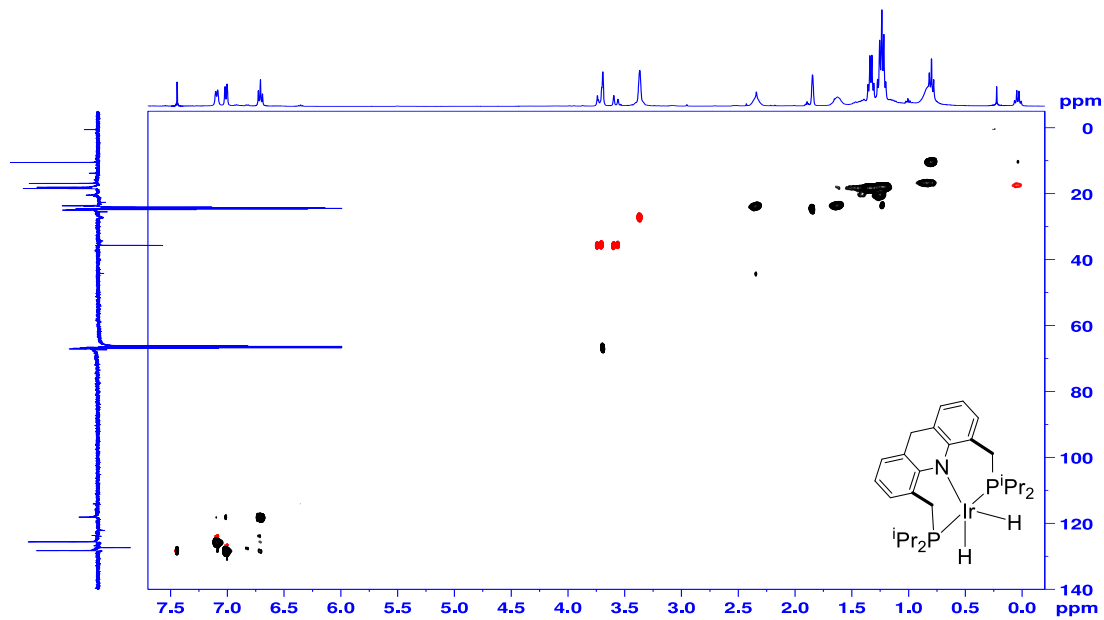


Figure S37. Complex 6 – ${}^{13}\text{C}$ - ${}^1\text{H}$ HSQC spectrum in THF- d_8 at -30 °C.

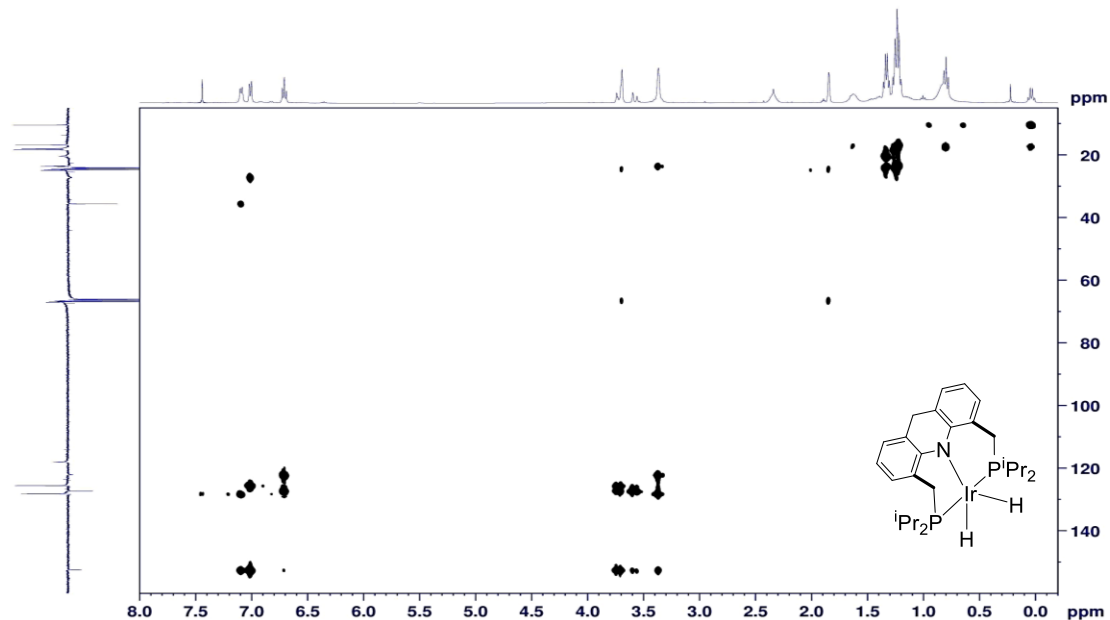


Figure S38. Complex 6 – ${}^{13}\text{C}$ - ${}^1\text{H}$ HMBC spectrum in THF- d_8 at -30 °C.

1.7 complex 7

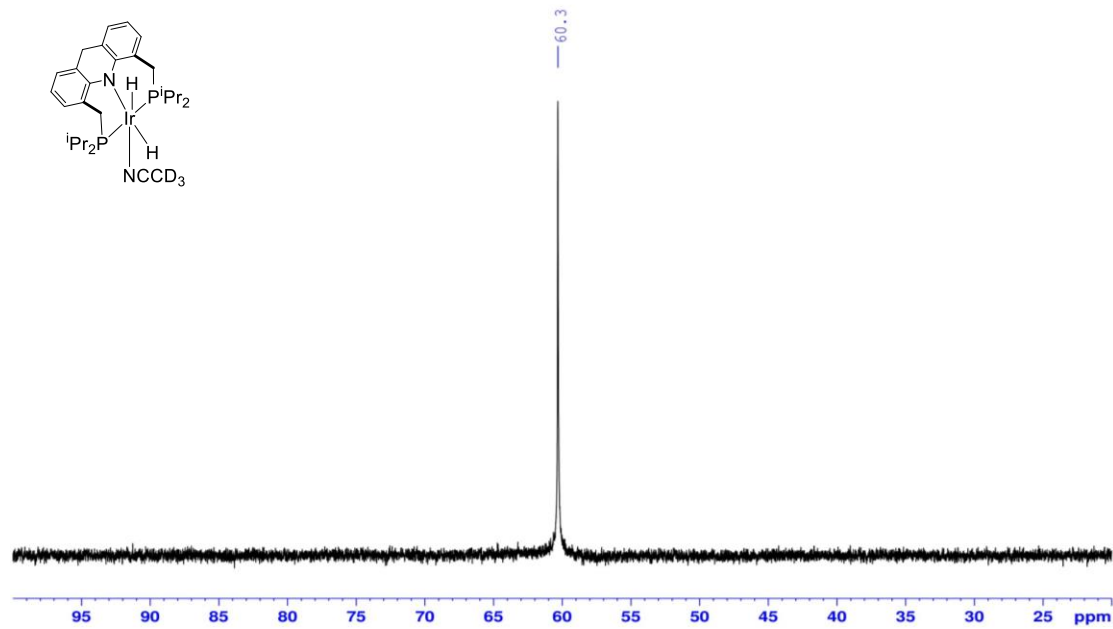


Figure S39. Complex 7 – $^{31}\text{P} \{^1\text{H}\}$ NMR spectrum in C_6D_6 .

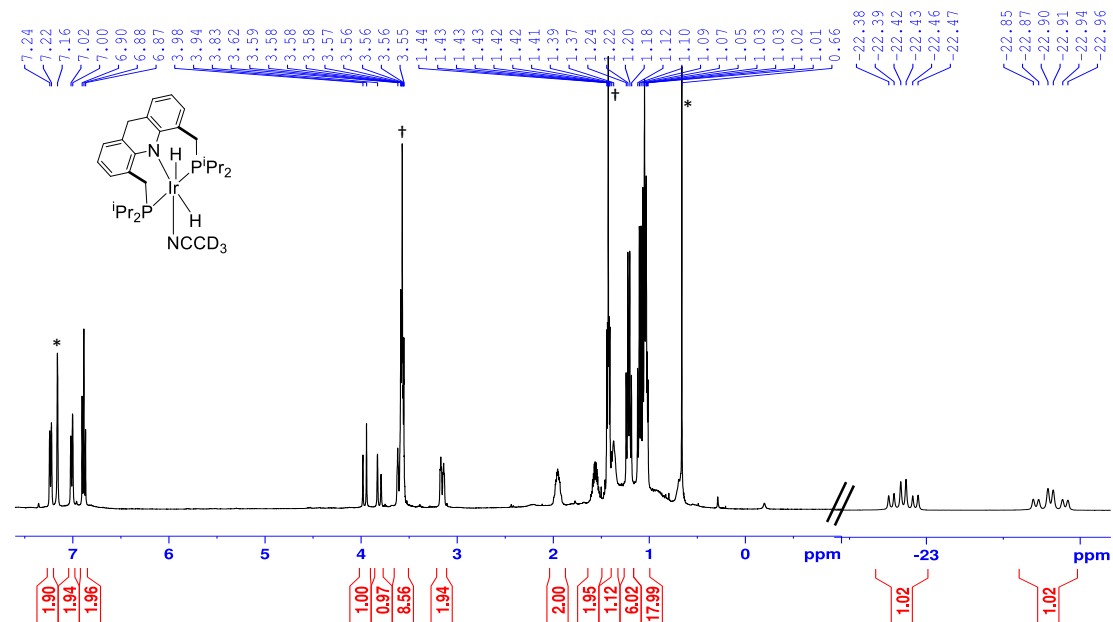


Figure S40. Complex 7 – ^1H NMR spectrum in C_6D_6 . * = residual solvent peak. † = residual THF.

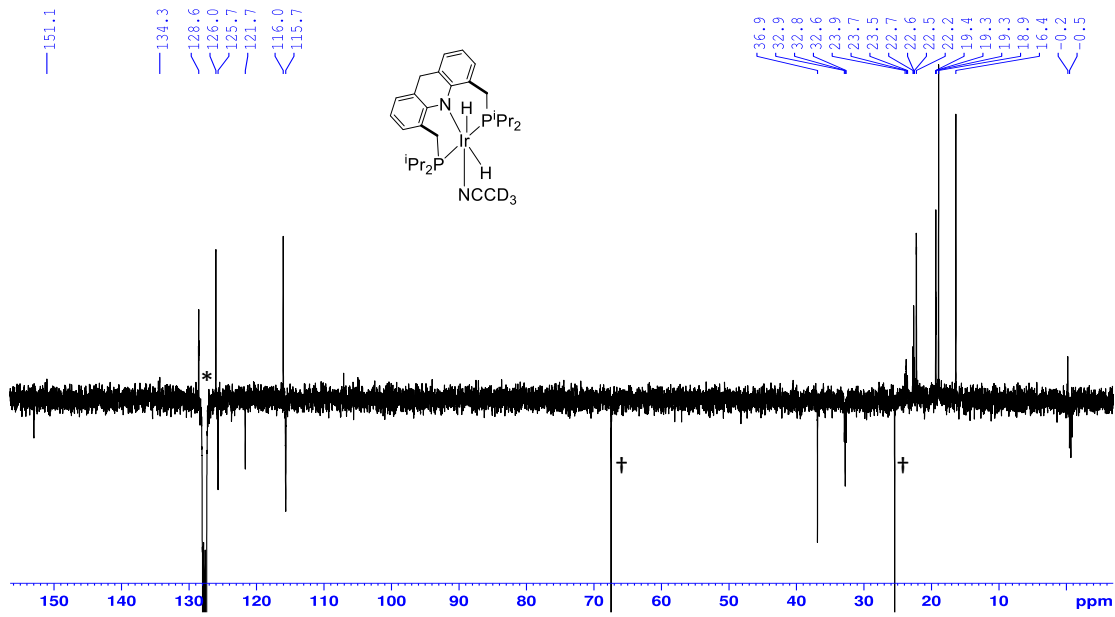


Figure S41. Complex 7 – ^{13}C DEPTQ spectrum in C_6D_6 . * = residual solvent peak. † = residual THF.

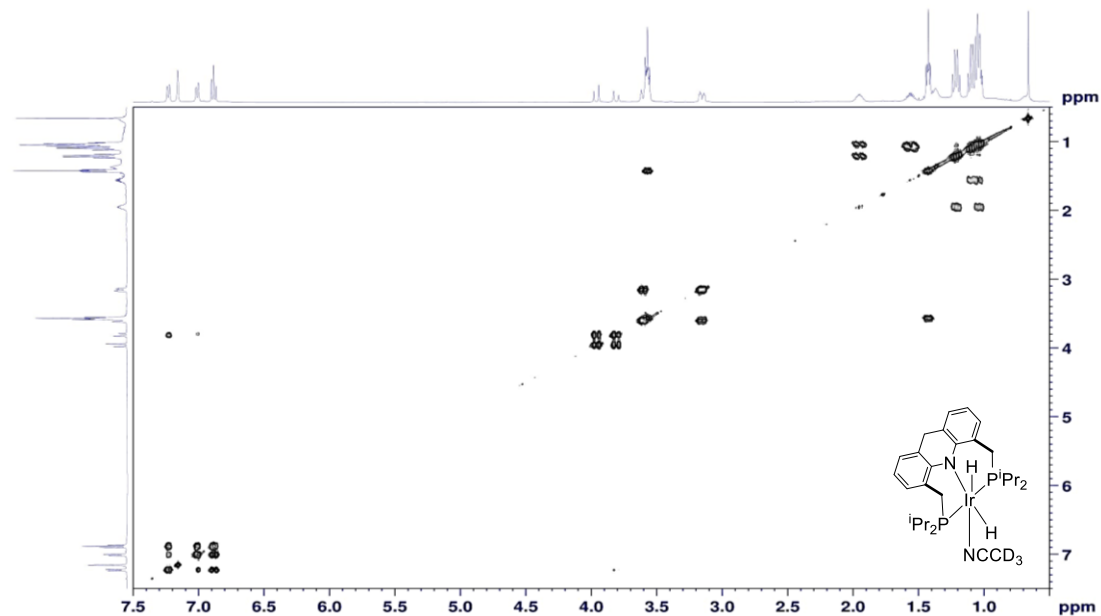


Figure S42. Complex 7 – ^1H COSY spectrum in C_6D_6 .

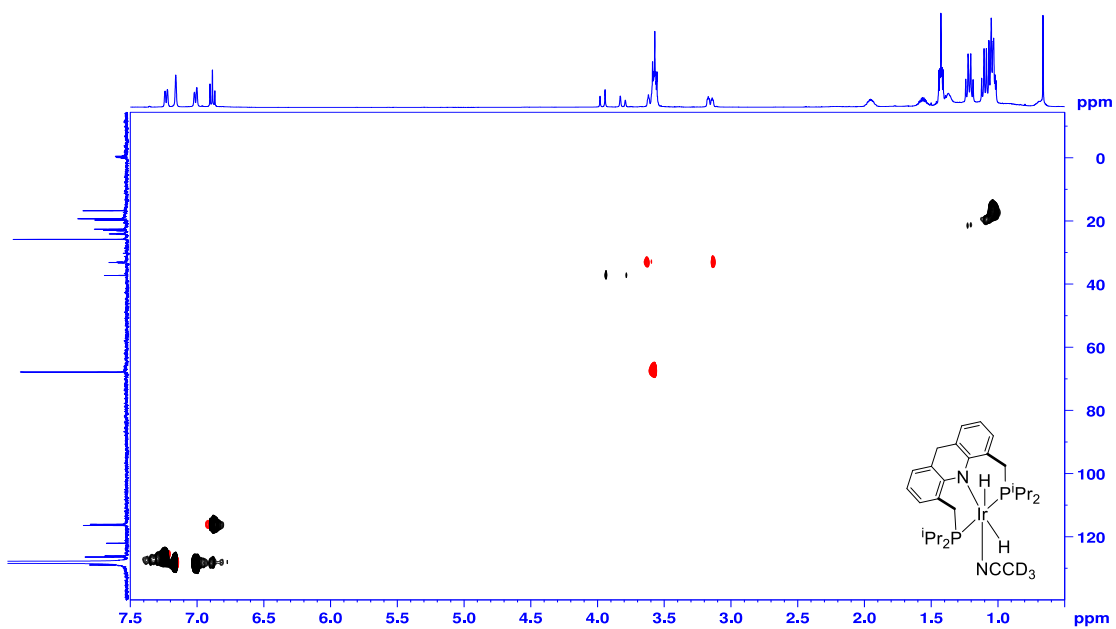


Figure S43. Complex 7 – ^{13}C - ^1H HSQC spectrum in C_6D_6 .

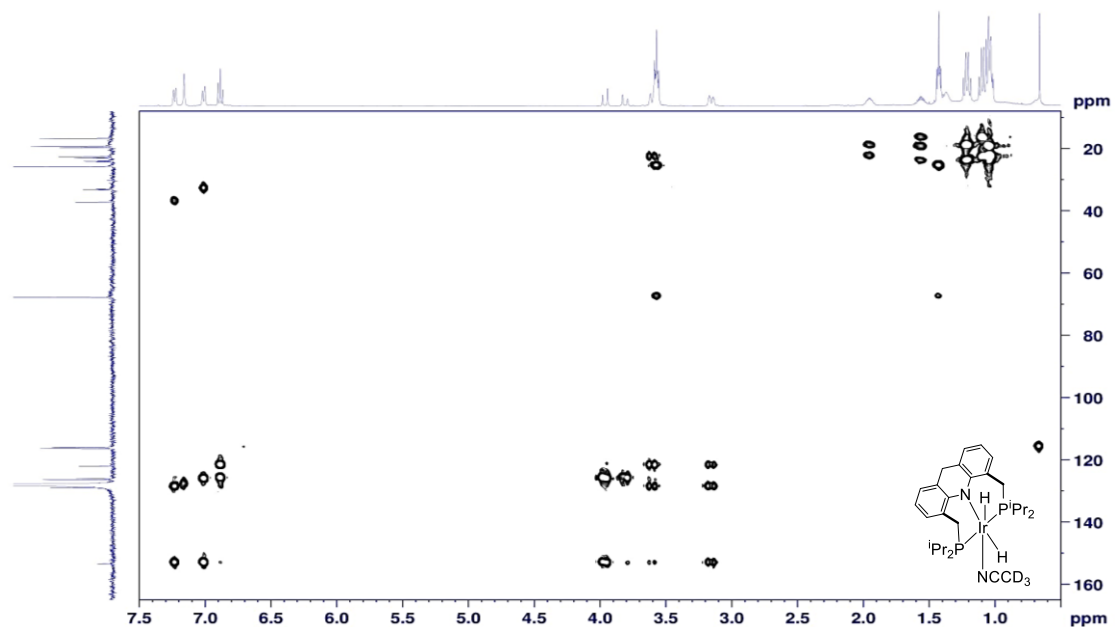


Figure S44. Complex 7 – ^{13}C - ^1H HMBC spectrum in C_6D_6 .

1.8 Complex 9

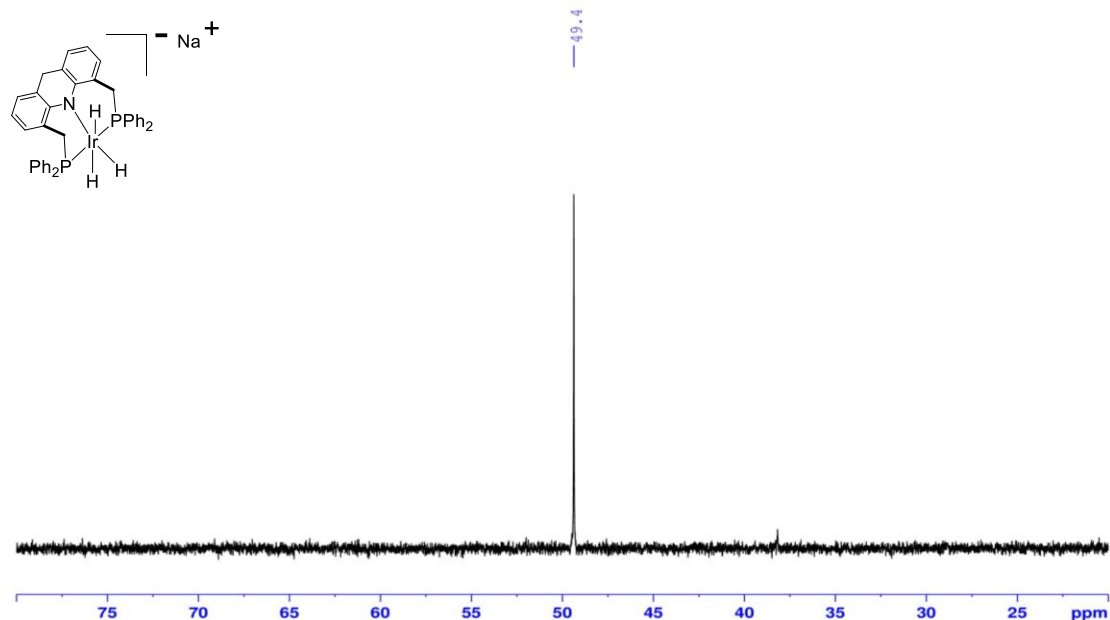


Figure S45. Complex 9 – ^{31}P - $\{{}^1\text{H}\}$ NMR spectrum in THF-d_8 at -20°C .

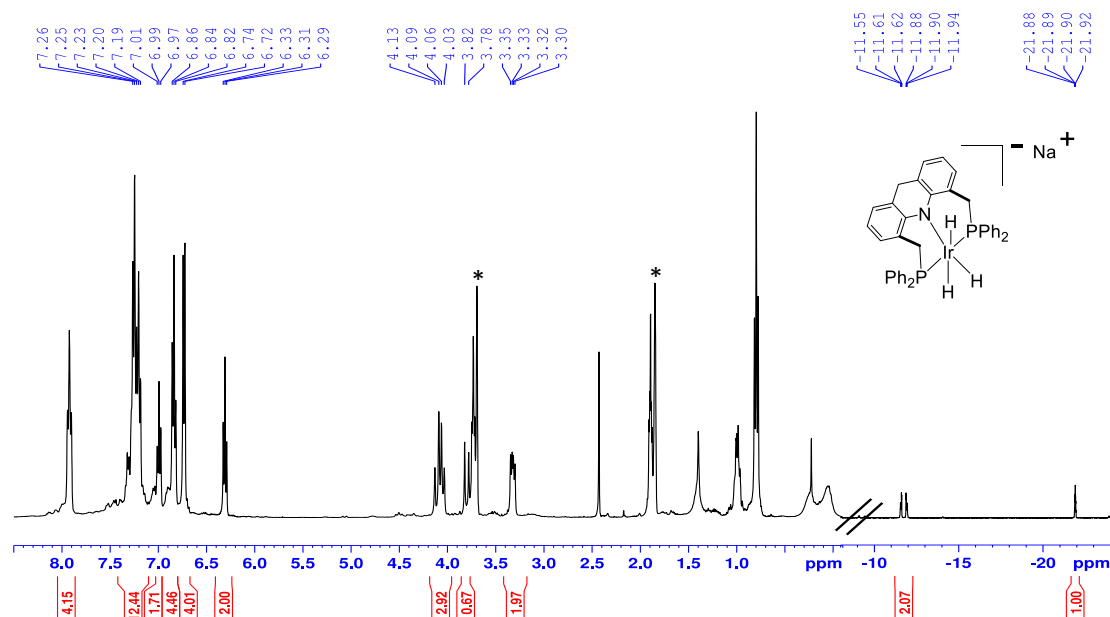


Figure S46. Complex 9 – ${}^1\text{H}$ NMR spectrum in THF-d_8 at -20°C . * = residual solvent peak.

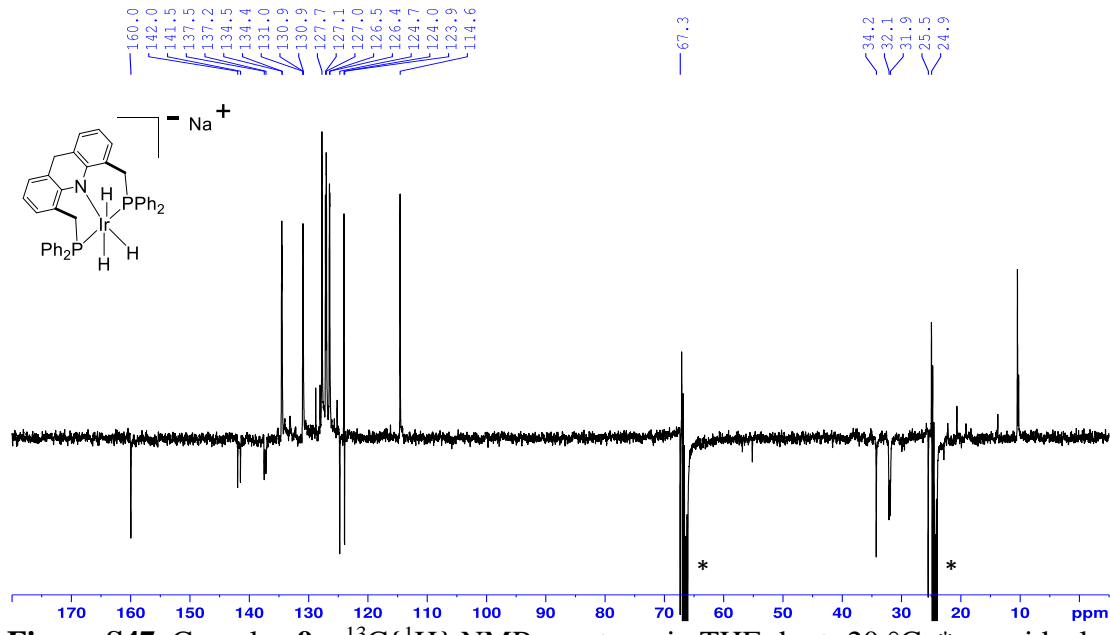


Figure S47. Complex **9** – $^{13}\text{C}\{^1\text{H}\}$ NMR spectrum in THF-d_8 at $-20\text{ }^\circ\text{C}$. * = residual solvent peak.

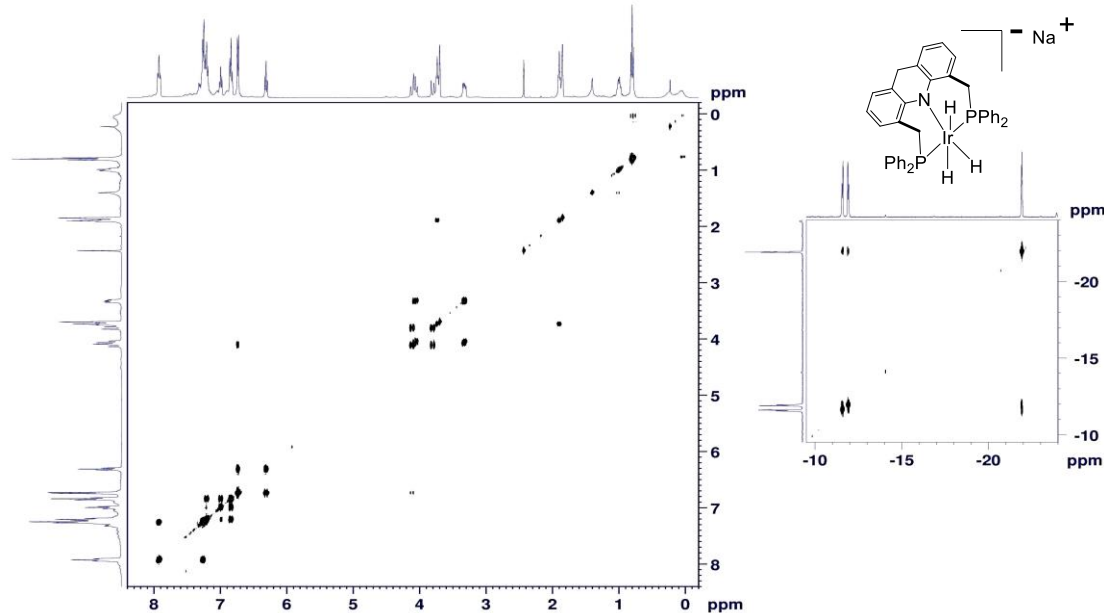


Figure S48. Complex **9** – ^1H COSY spectrum in THF-d_8 at $-20\text{ }^\circ\text{C}$. Left image: 0 to 8.5 ppm. Right image: -25 to -10 ppm.

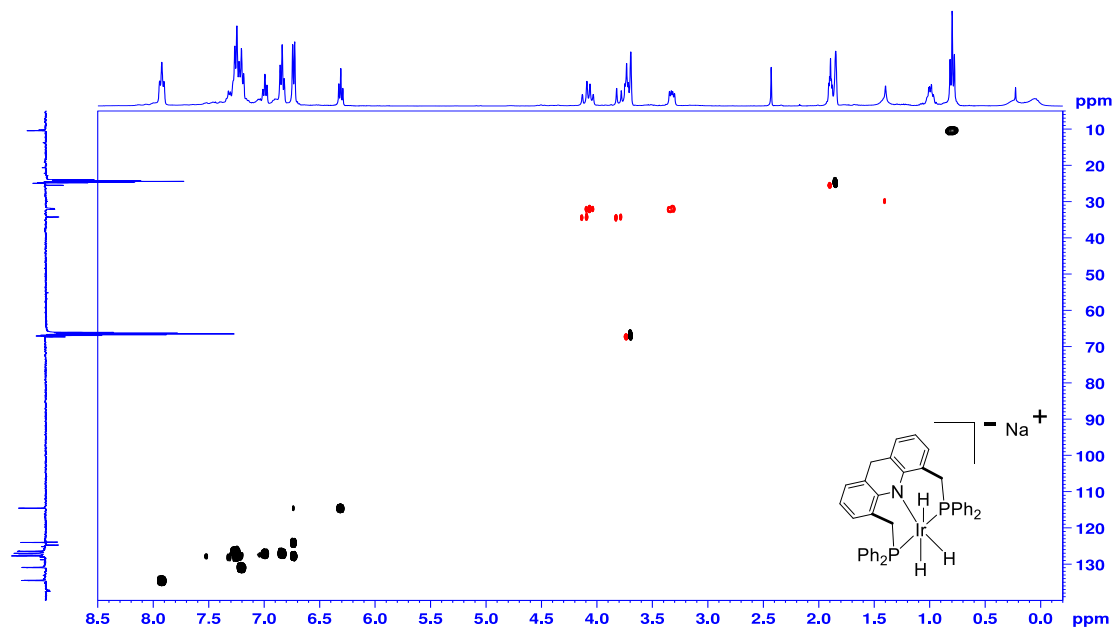


Figure S49. Complex **9** – ^{13}C - ^1H HSQC spectrum in THF-d_8 at -20°C .

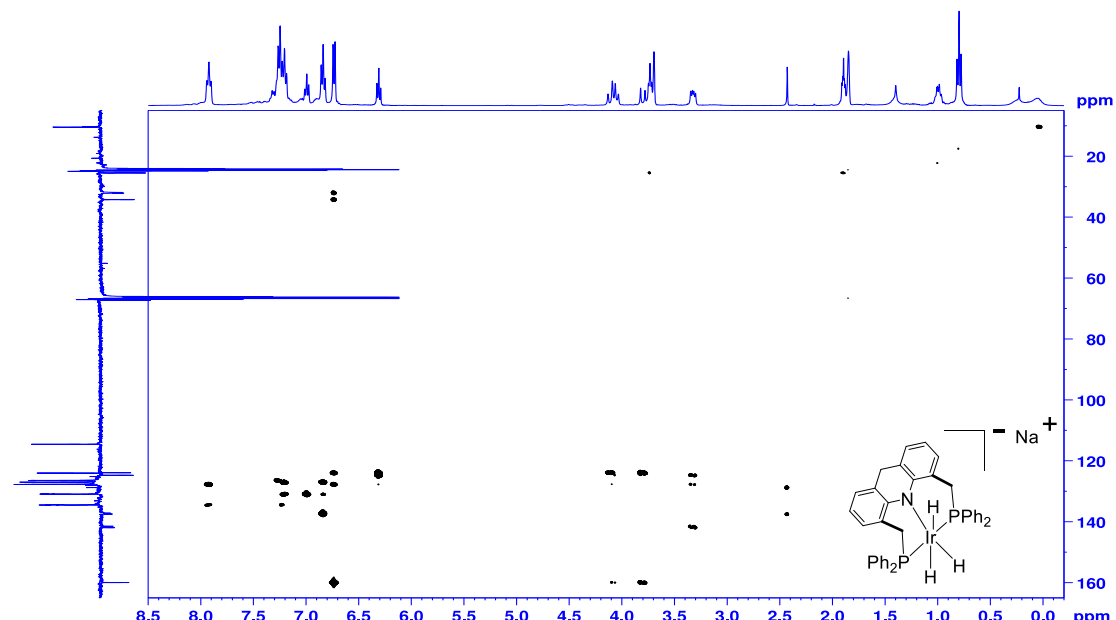


Figure S50. Complex **9** – ^{13}C - ^1H HMBC spectrum in THF-d_8 at -20°C .

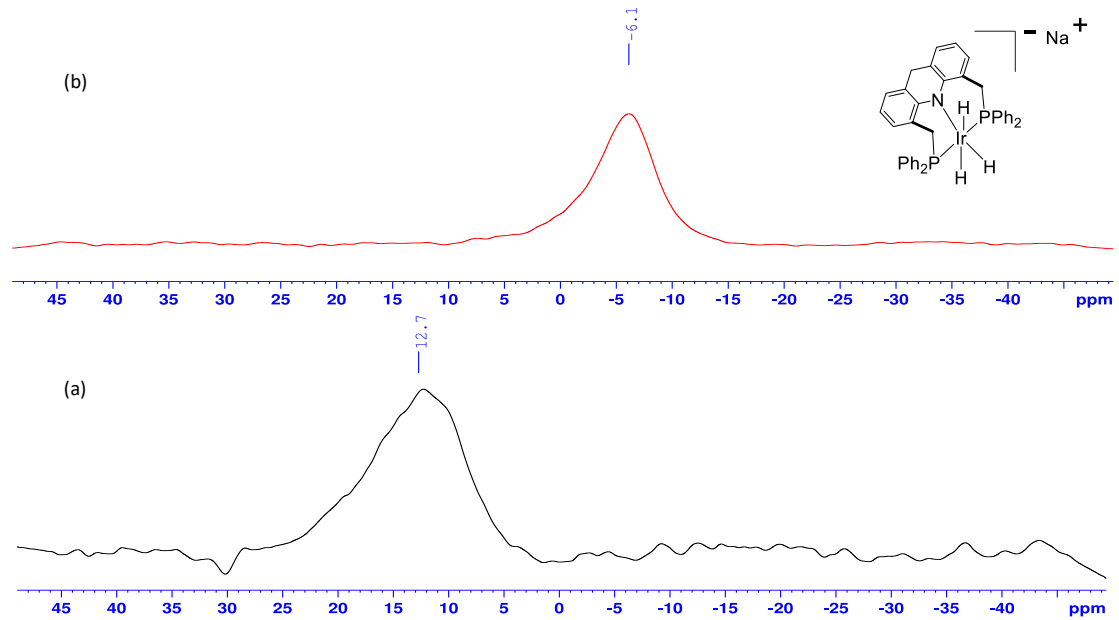


Figure S51. Complex **9** – ^{23}Na NMR spectra in THF at room temperature. (a) Pristine complex in THF. (b) After addition of 0.6 equiv of 18-crown-6.

1.9 Complex 10

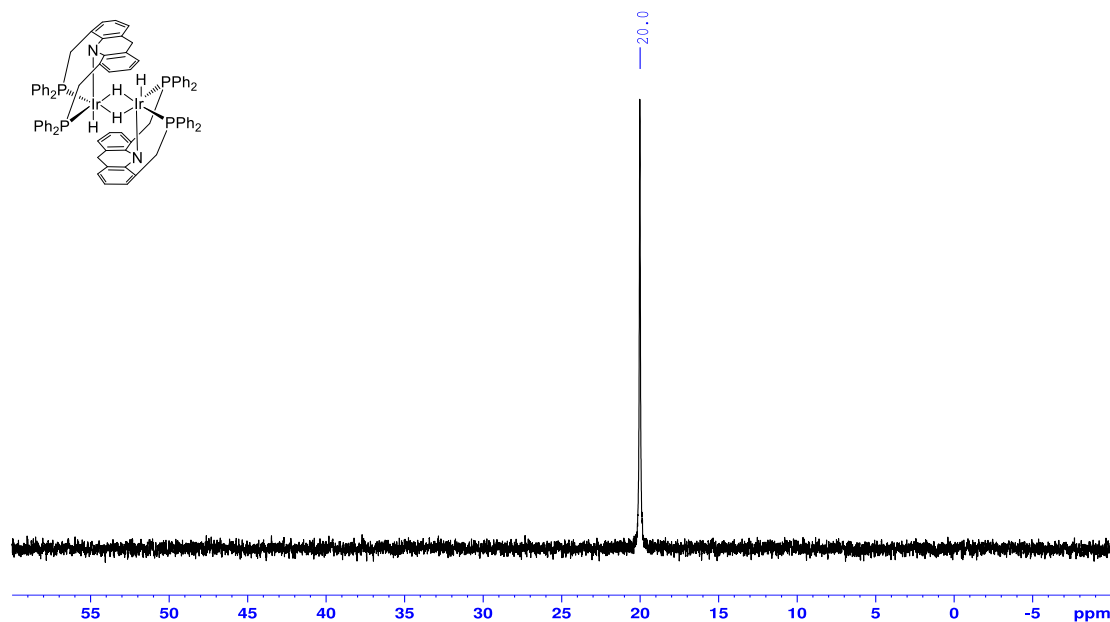


Figure S52. Complex 10 – ³¹P{¹H} NMR spectrum in C₆D₆.

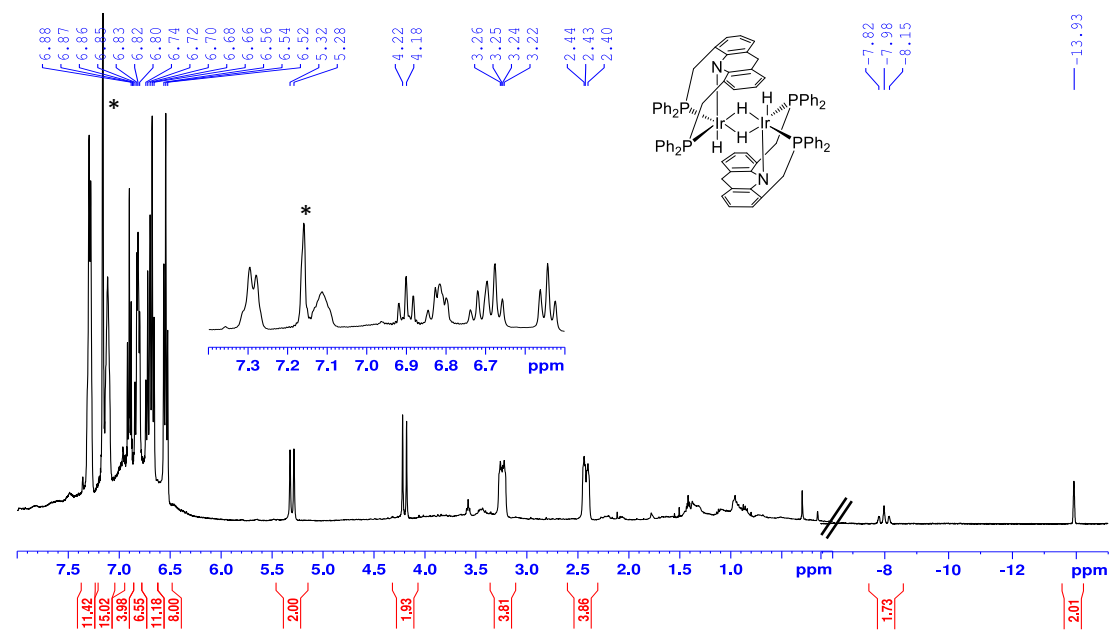


Figure S53 . Complex 10 – ¹H NMR spectrum in C₆D₆. * = residual solvent peak.

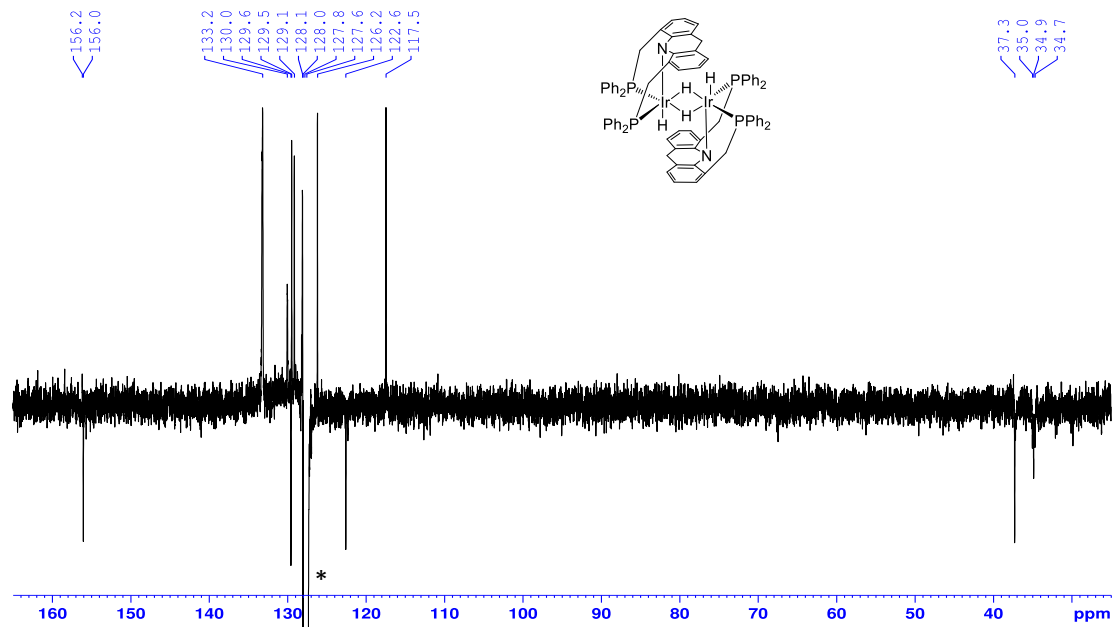


Figure S54. Complex **10** – $^{13}\text{C}\{^1\text{H}\}$ NMR spectrum in C_6D_6 . * = residual solvent peak.

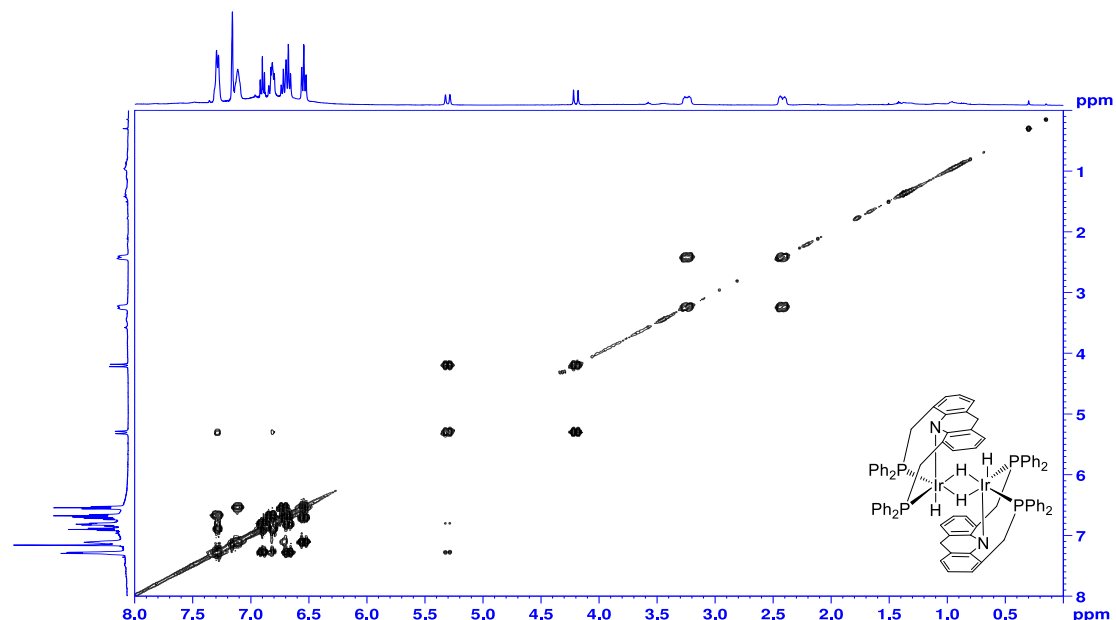


Figure S55. Complex **10** – ^1H - COSY spectrum in C_6D_6 .

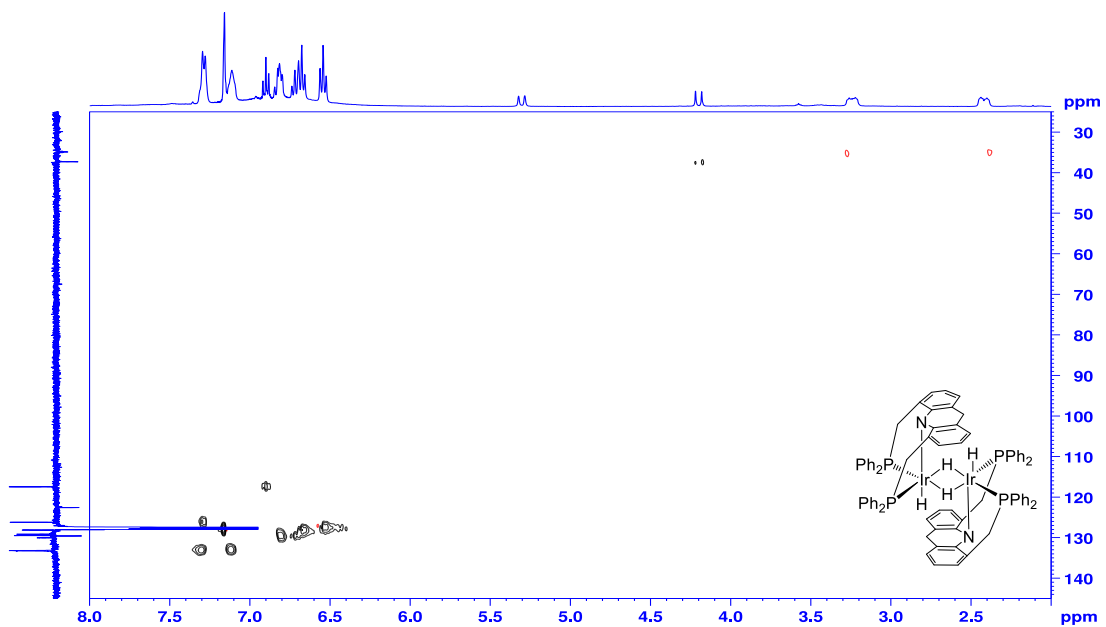


Figure S56. Complex **10** – ^{13}C - ^1H HSQC spectrum in C_6D_6 .

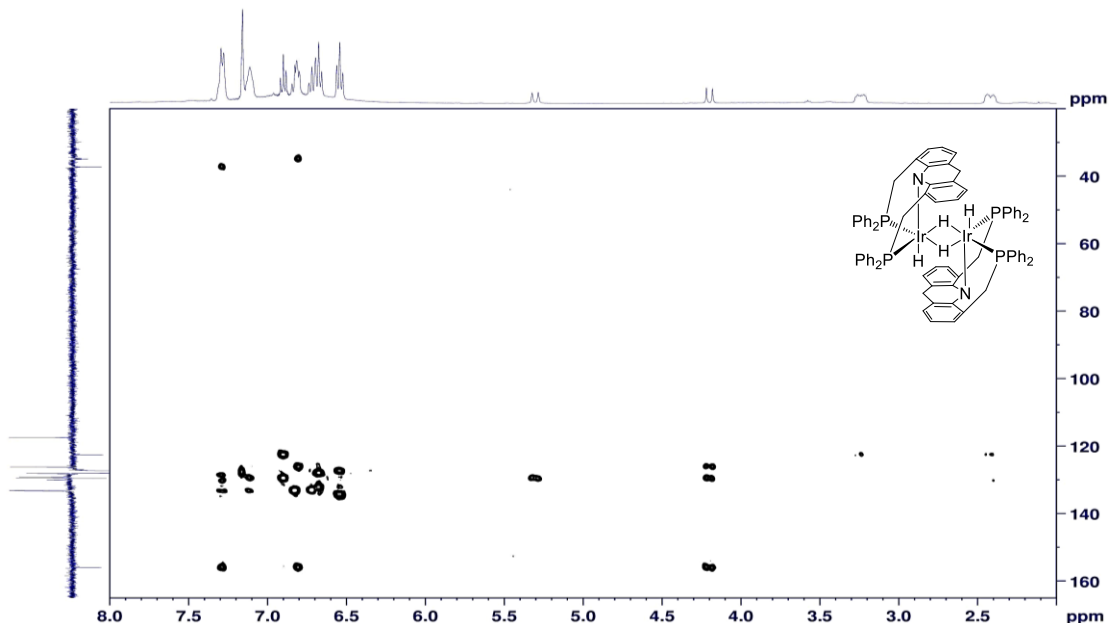


Figure S57. Complex **10** – ^{13}C - ^1H HMBC spectrum in C_6D_6 .

1.10 Complex 11

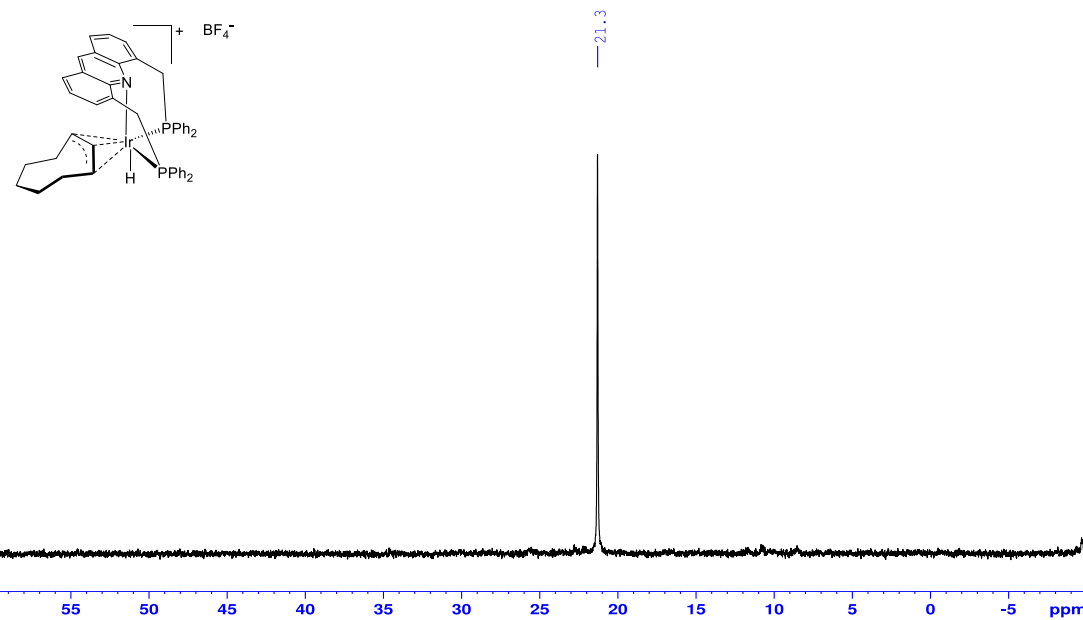


Figure S58. Complex 11 – $^{31}\text{P}\{^1\text{H}\}$ NMR spectrum in acetone- d_6 .

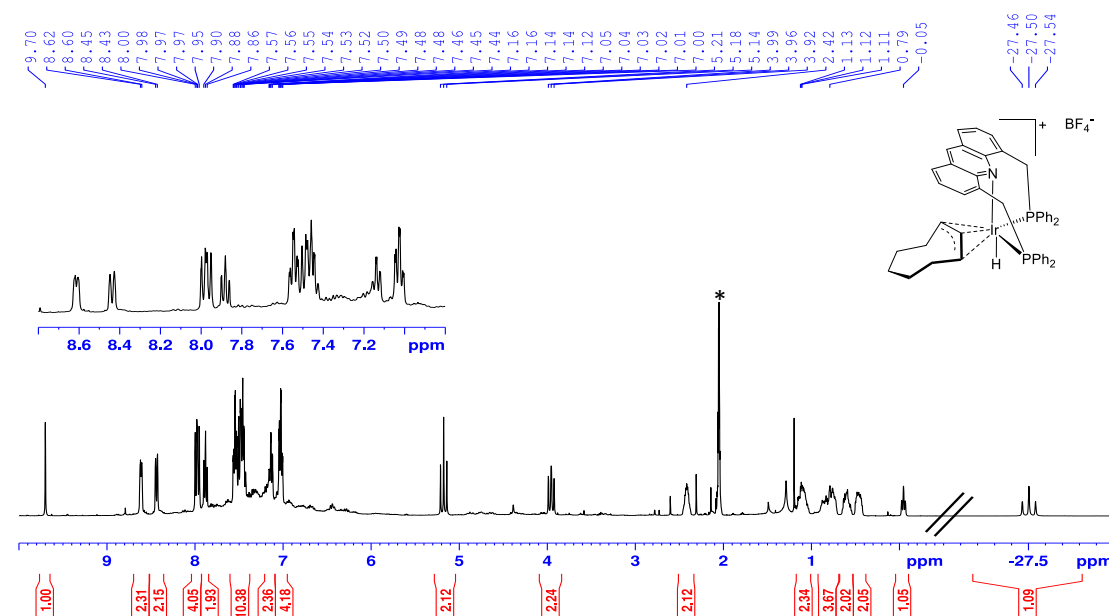


Figure S59. Complex 11 – ^1H NMR spectrum in acetone- d_6 . * = residual solvent peak.

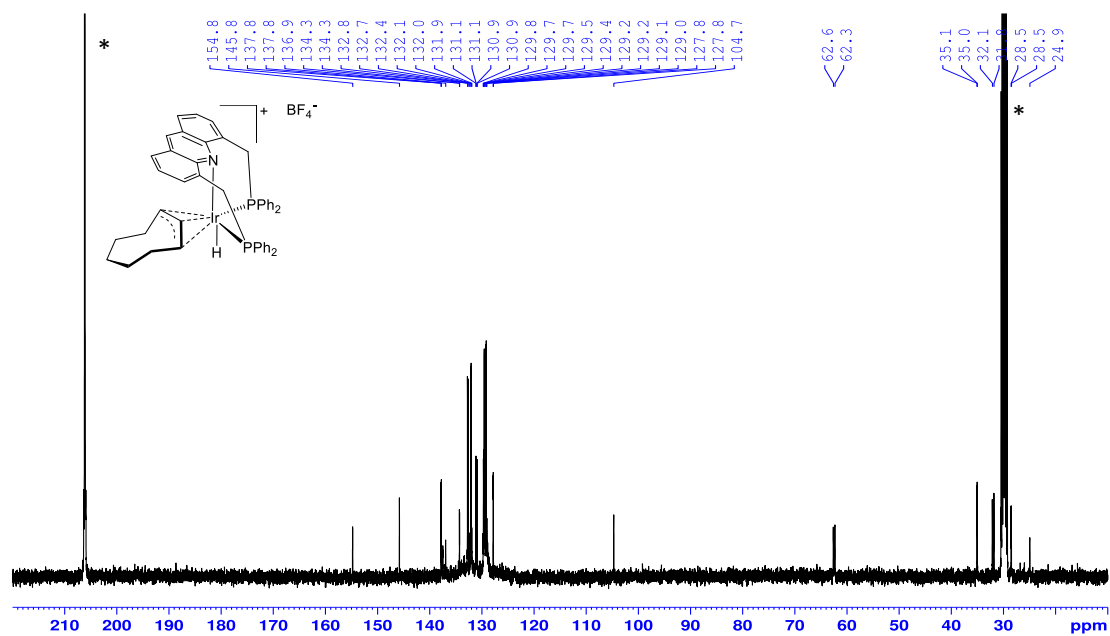


Figure S60. Complex **11** – $^{13}\text{C}\{^1\text{H}\}$ NMR spectrum in acetone- d_6 . * = residual solvent peak.

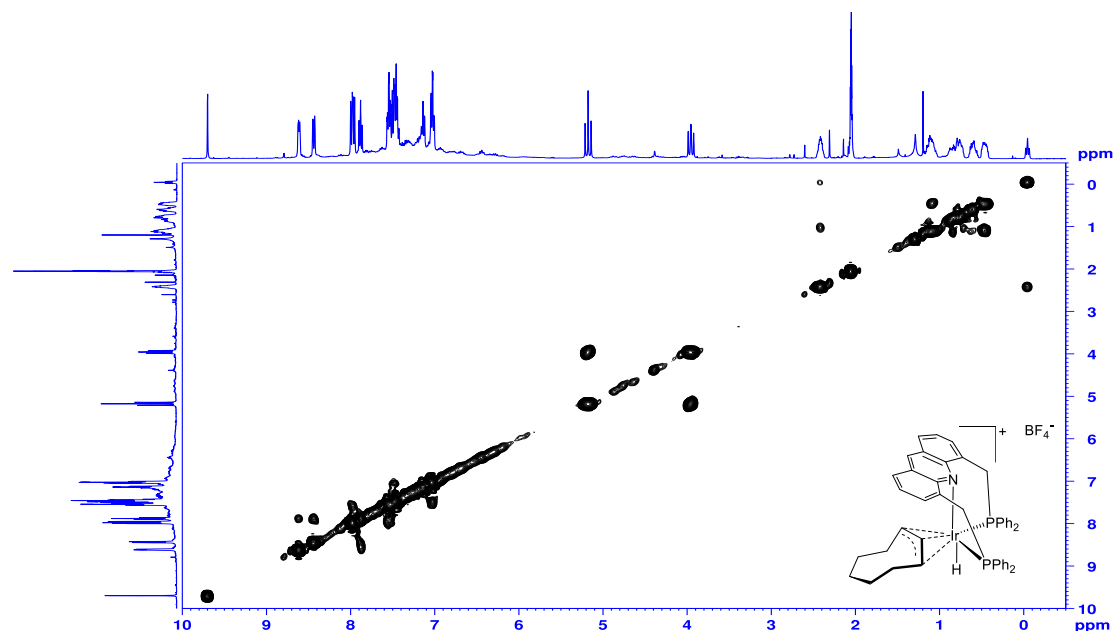


Figure S61. Complex **11** – ^1H COSY spectrum in acetone- d_6 .

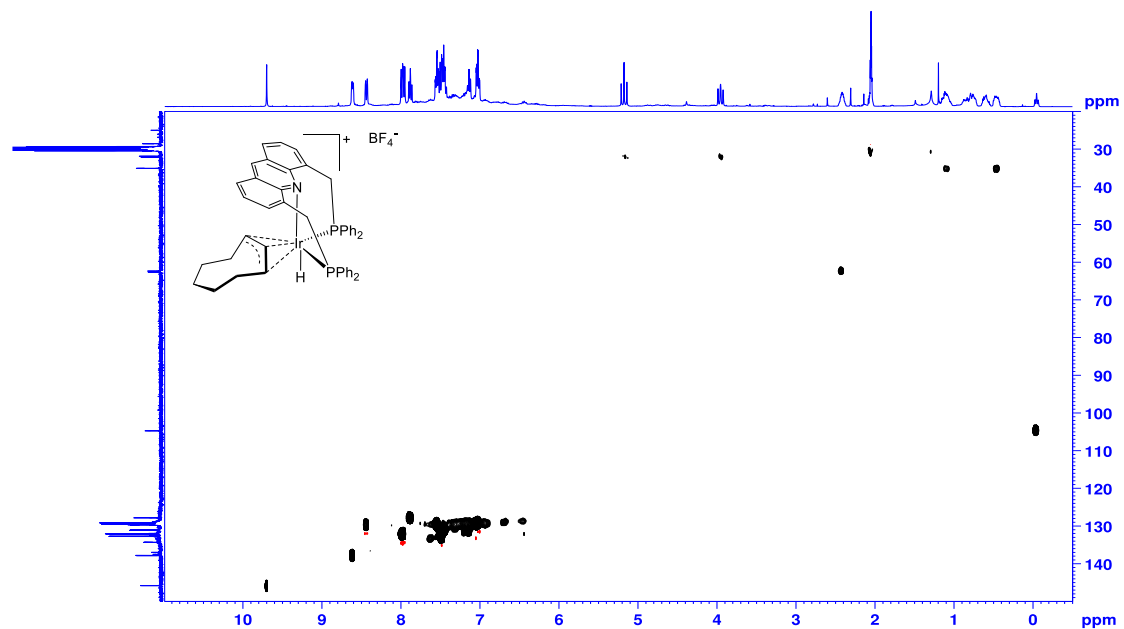


Figure S62. Complex **11** – ^{13}C - ^1H HSQC spectrum in acetone- d_6 .

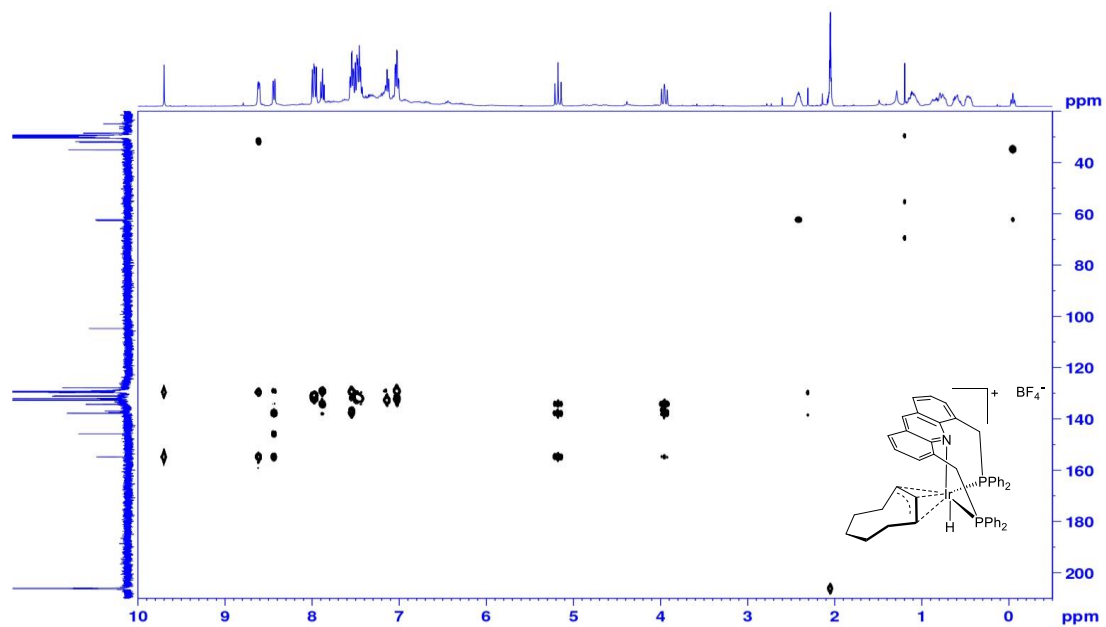


Figure S63. Complex **11** – ^{13}C - ^1H HMBC spectrum in acetone- d_6 .

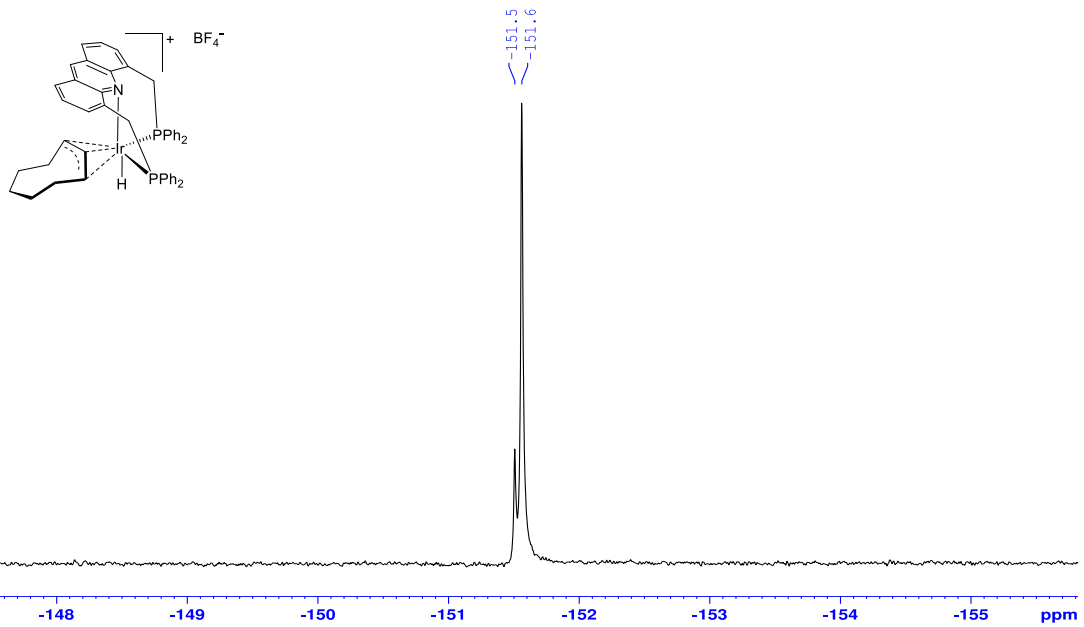


Figure S64. Complex **11** – ${}^{19}\text{F}\{{}^1\text{H}\}$ NMR spectrum in acetone- d_6

1.11 Complex 12

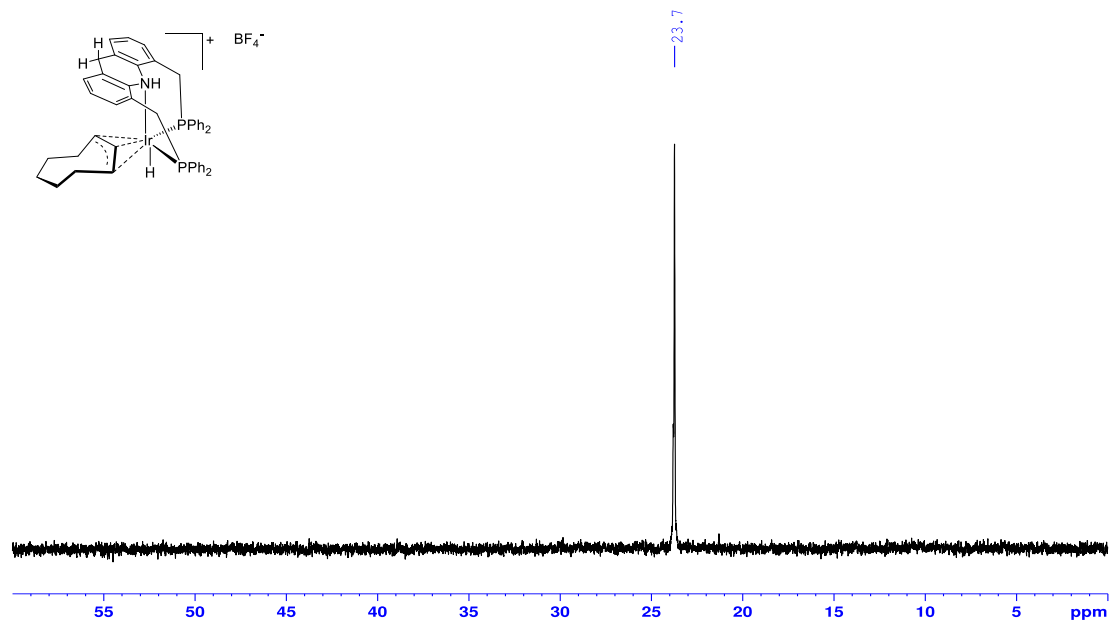


Figure S65. Complex 12 – ³¹P{¹H} NMR spectrum in acetone-d₆.

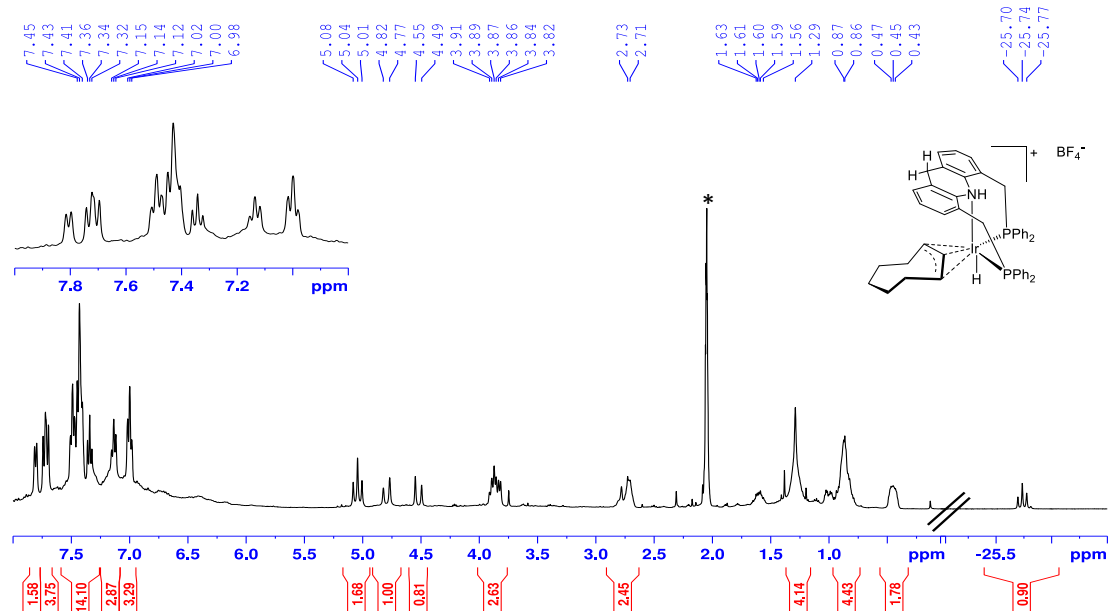


Figure S66. Complex 12 – ¹H NMR spectrum in acetone-d₆. * = residual solvent peak.

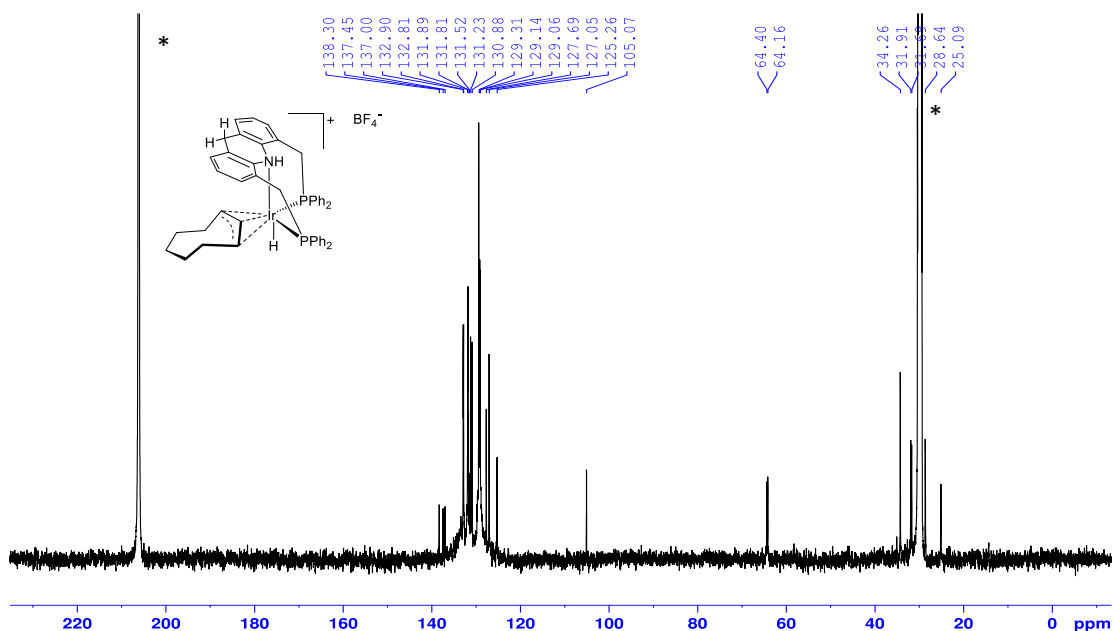


Figure S67. Complex **12** – $^{13}\text{C}\{^1\text{H}\}$ NMR spectrum in acetone- d_6 . * = residual solvent peak.

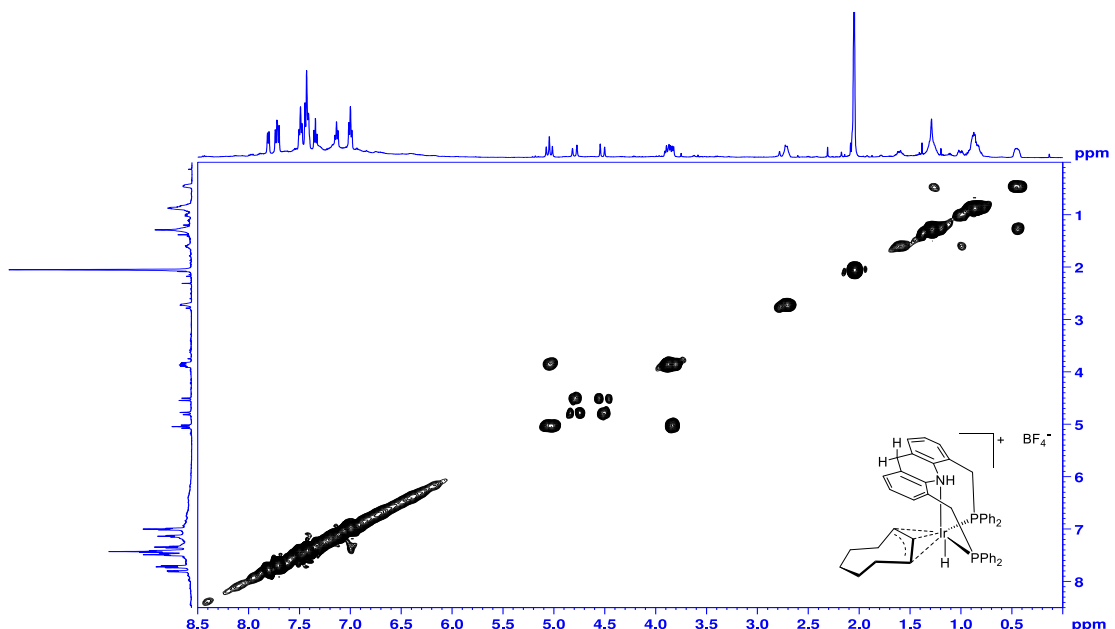


Figure S68. Complex **12** – ^1H COSY spectrum in acetone- d_6 .

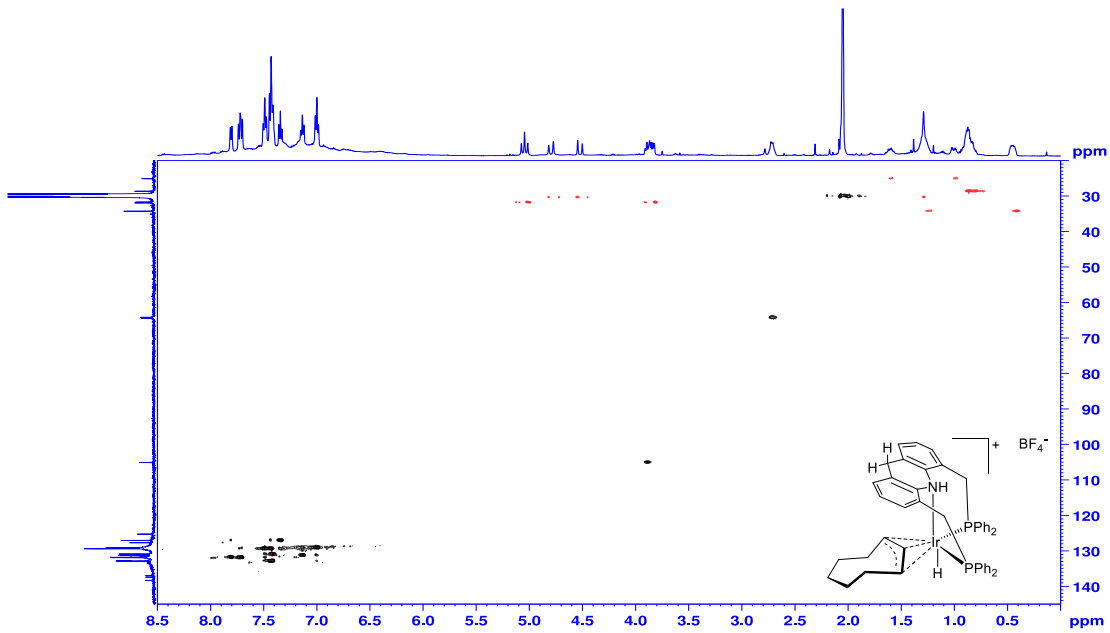


Figure S69. Complex 12 – ^{13}C - ^1H HSQC spectrum in acetone- d_6 .

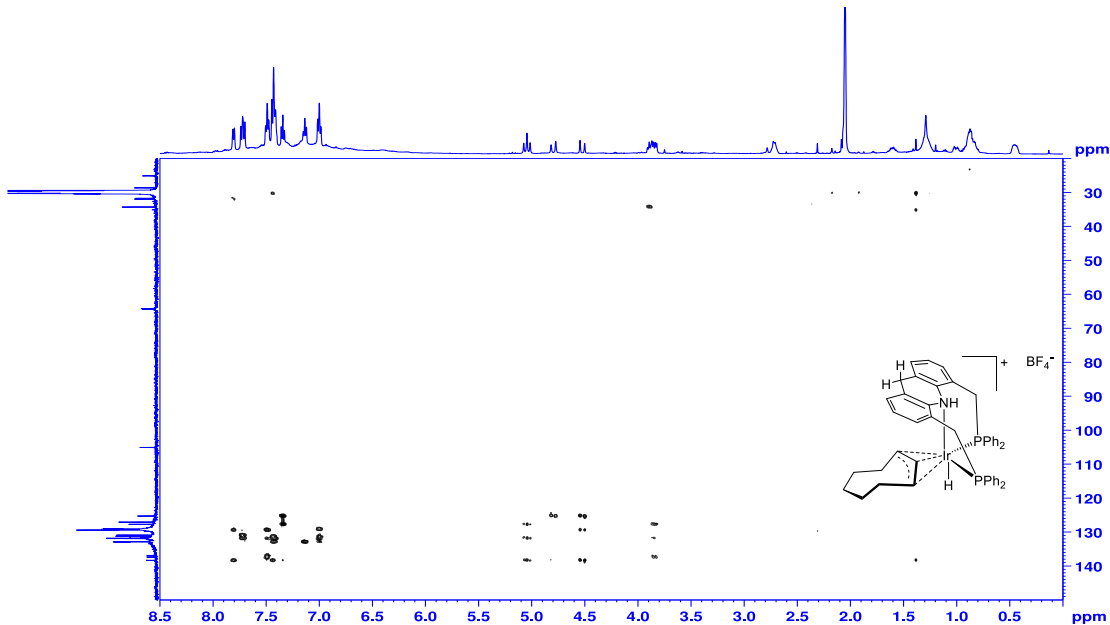


Figure S70. Complex 12 – ^{13}C - ^1H HMBC spectrum in acetone- d_6 .

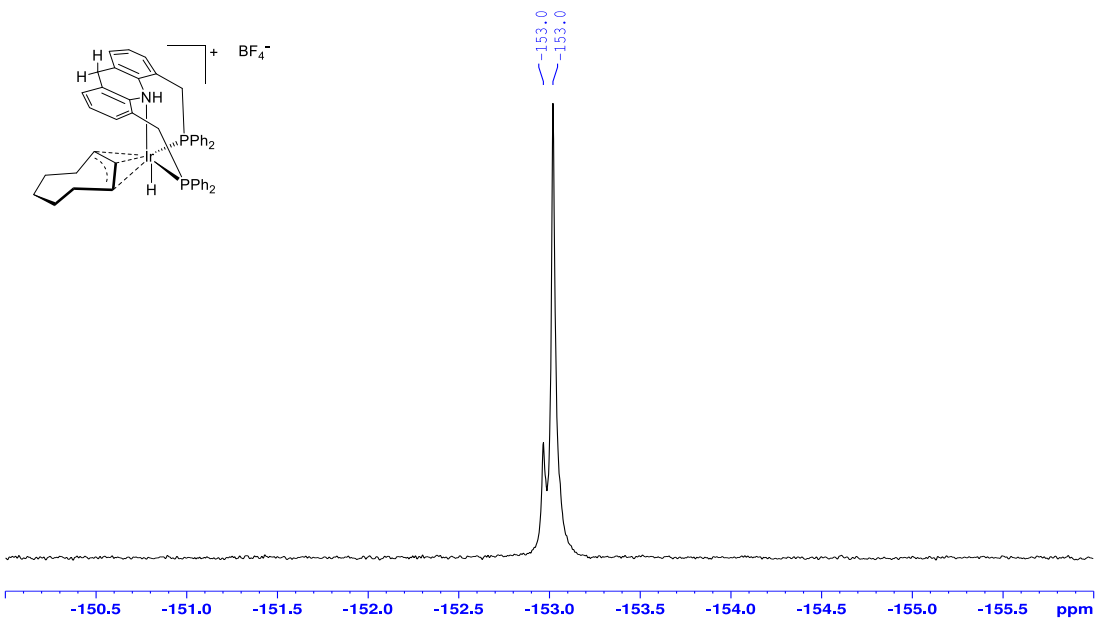


Figure S71. Complex **12** – ¹⁹F{¹H} NMR spectrum in acetone-d₆.

1.12 Complex 13

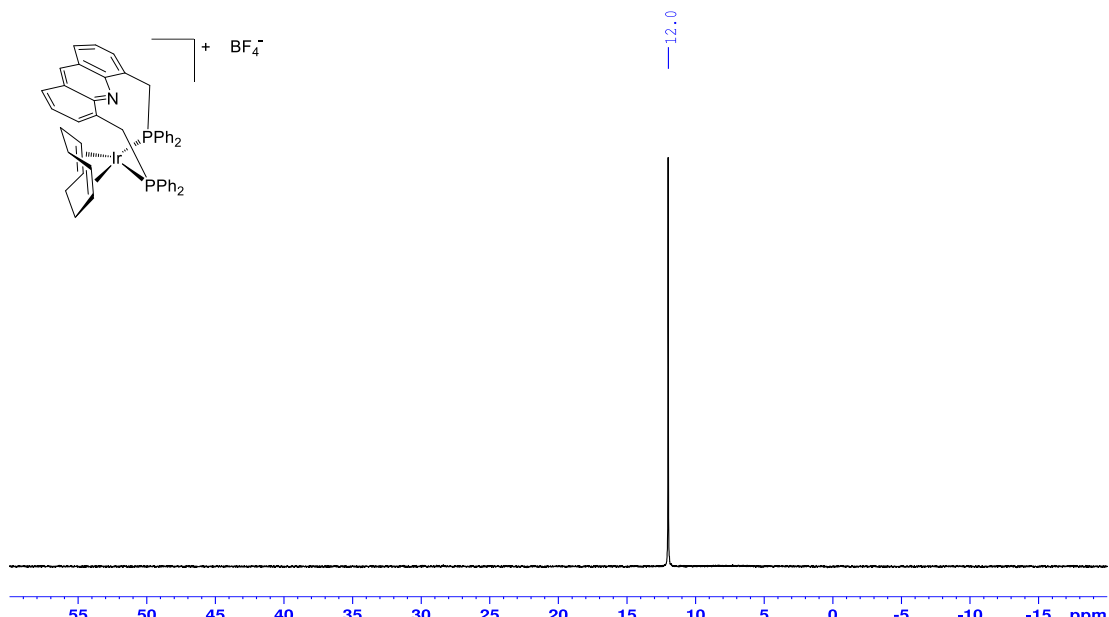


Figure S72. Complex 13 – $^{31}\text{P}\{\text{H}\}$ NMR spectrum in acetone- d_6 .

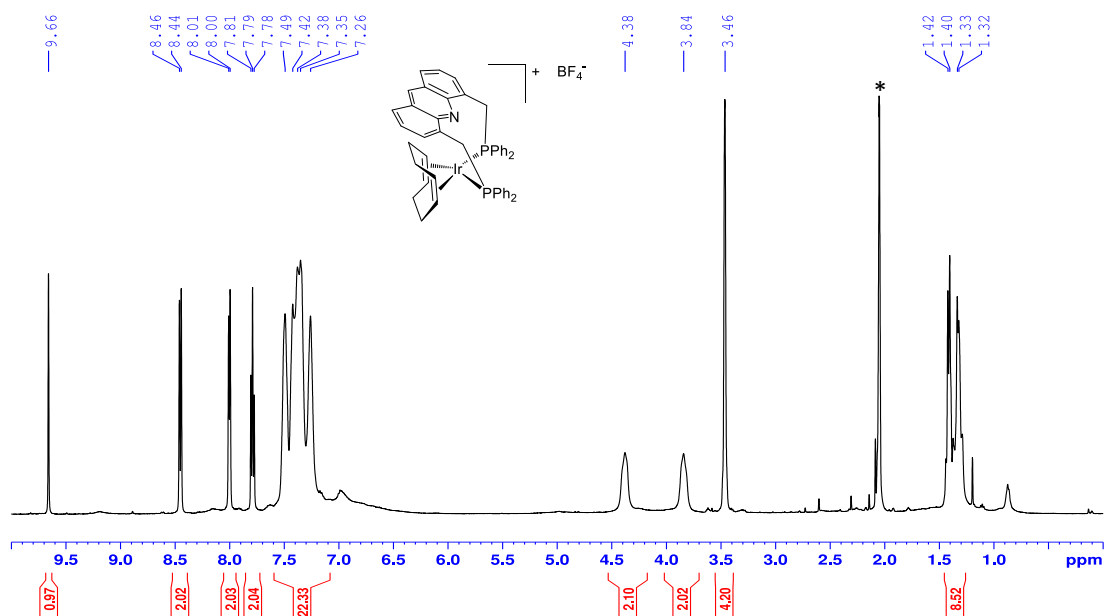


Figure S73. Complex 13 – ^1H NMR spectrum in acetone- d_6 . * = residual solvent peak.

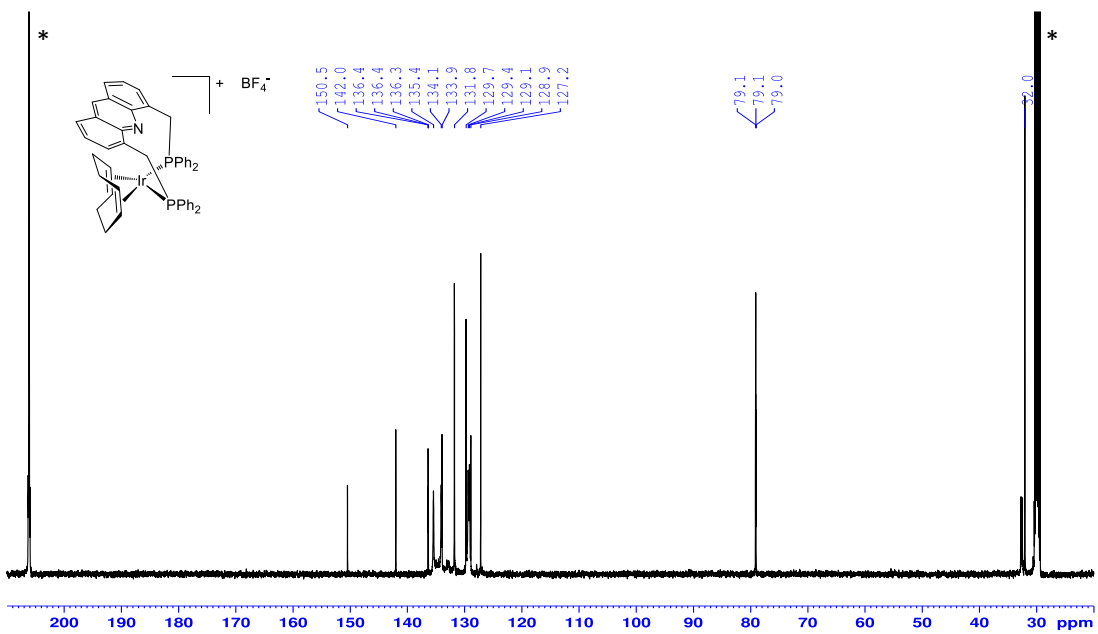


Figure S74. Complex **13** – $^{13}\text{C}\{^1\text{H}\}$ NMR spectrum in acetone- d_6 . * = residual solvent peak.

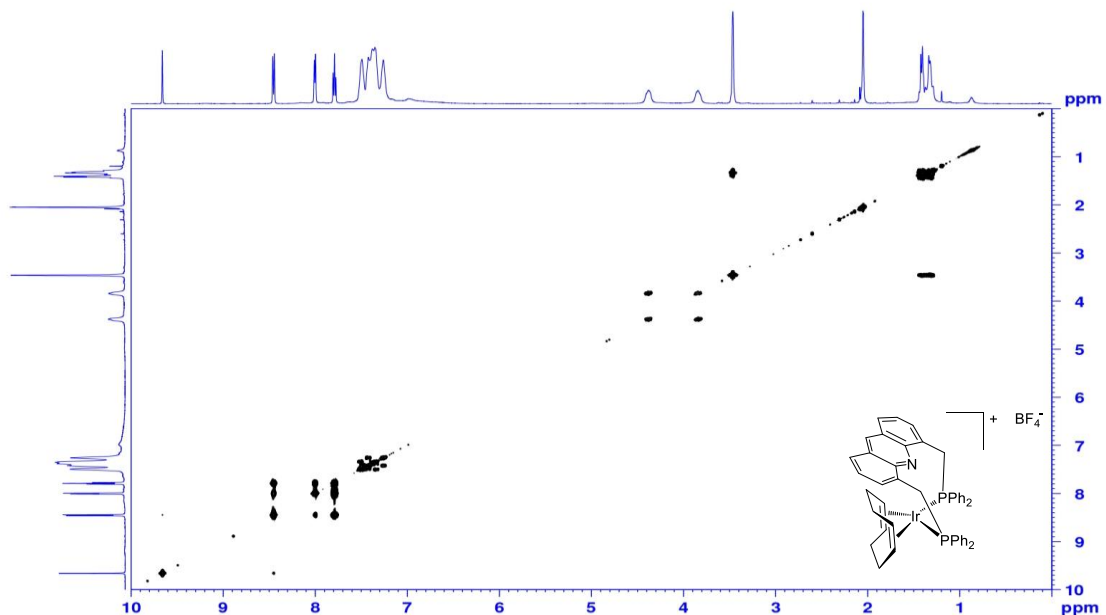


Figure S75. Complex **13** – ^1H COSY spectrum in acetone- d_6 .

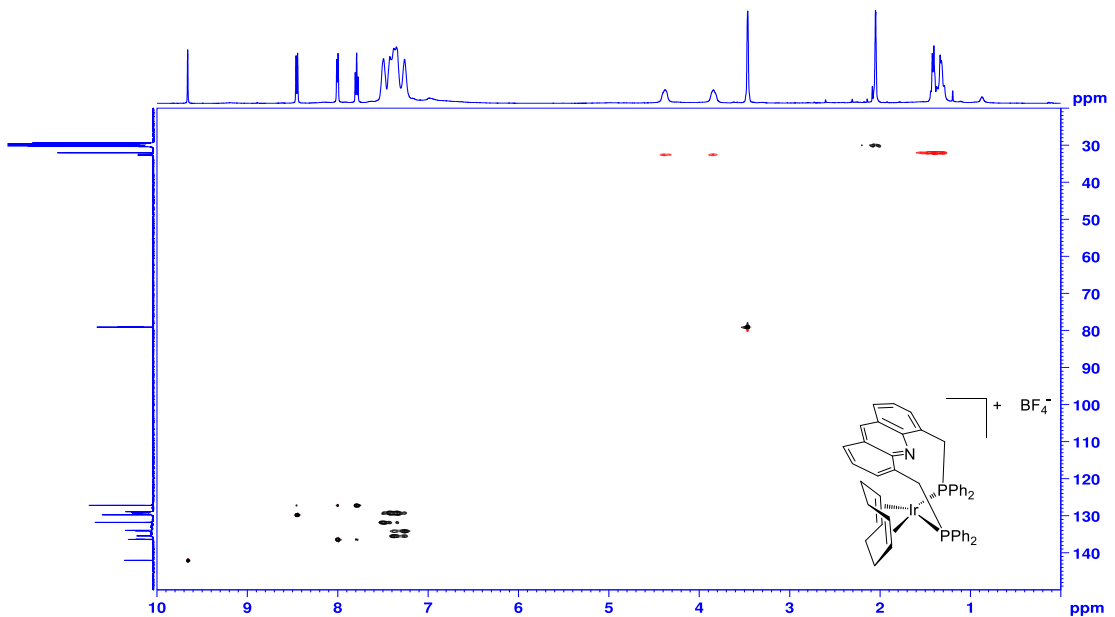


Figure S76. Complex **13** – ^{13}C - ^1H HSQC spectrum in acetone- d_6 .

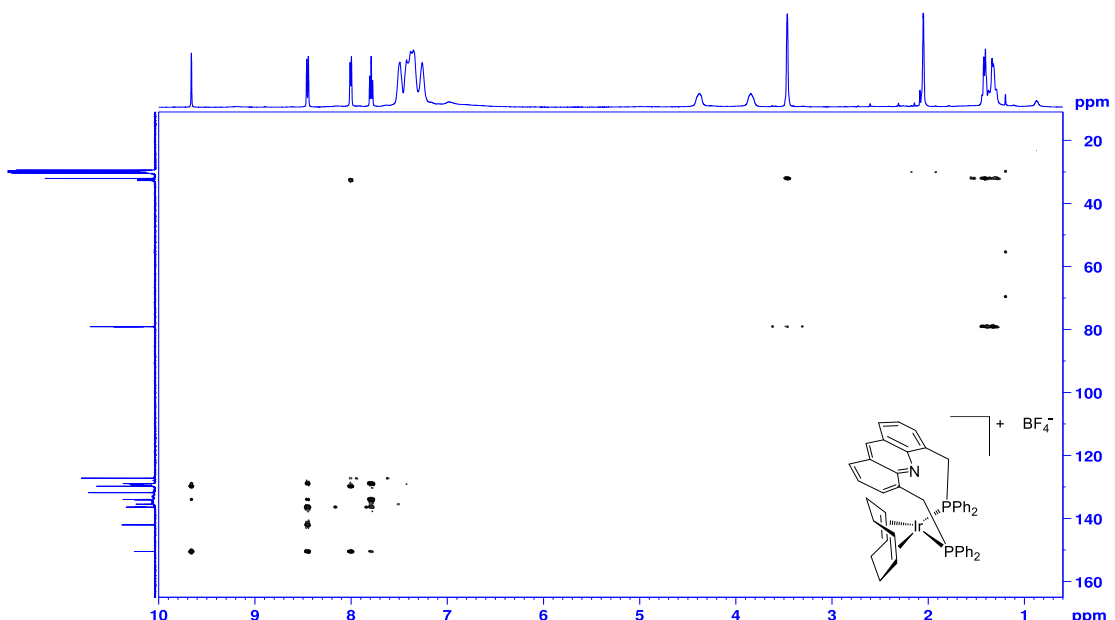


Figure S77. Complex **13** – ^{13}C - ^1H HMBC spectrum in acetone- d_6 .

2. Diffusion-ordered NMR spectroscopy measurements for complexes **3, **6** and **10****

A 10 mM solution of each complex - **3**, **6** and **10** - was prepared in THF-d₈/THF (1:5.6 v/v), and was subjected to a diffusion-ordered ¹H NMR spectroscopy (¹H-DOSY) experiment. The extracted diffusion coefficients were corrected based on the reported coefficient for nondeuterated THF.

The corrected diffusion coefficients are as follows:

Complex **3**: $0.918 \pm 0.006 \times 10^{-9} \text{ m}^2/\text{s}$

Complex **6**: $0.953 \pm 0.002 \times 10^{-9} \text{ m}^2/\text{s}$

Complex **10**: $0.606 \pm 0.006 \times 10^{-9} \text{ m}^2/\text{s}$

3. IR spectra

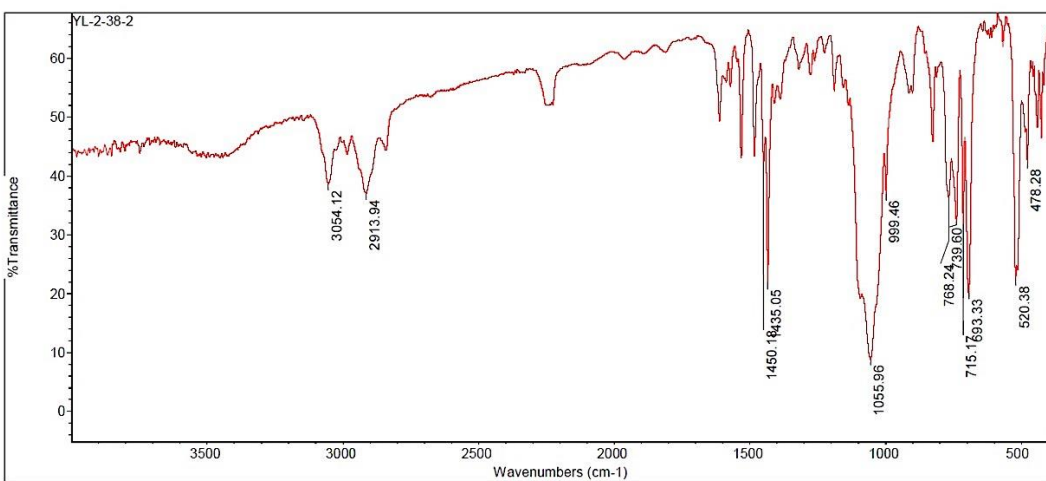


Figure S78. IR spectrum of complex 11 (KBr).

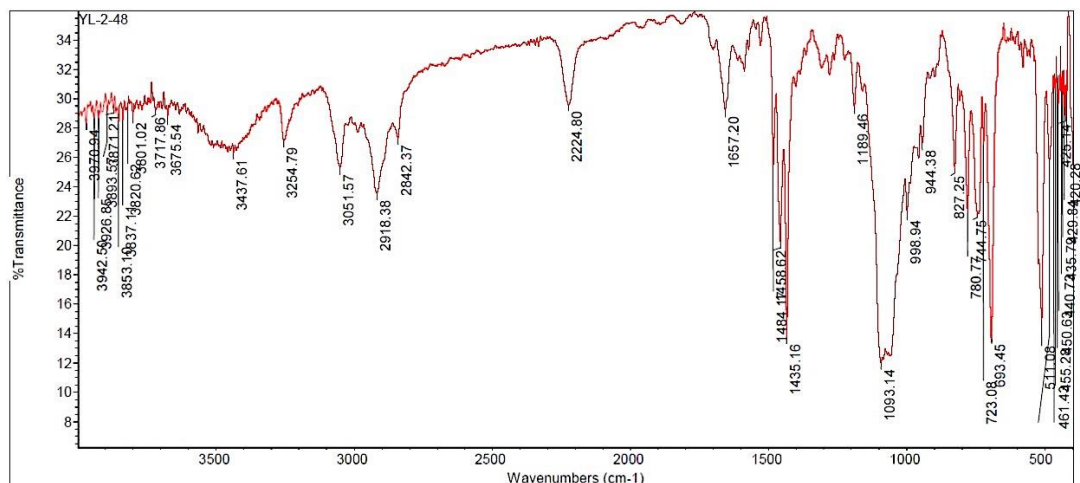


Figure S79. IR spectrum of complex 12 (KBr).

4. GC-TCD measurement for gas phase in the formation of complexes 5 and 6

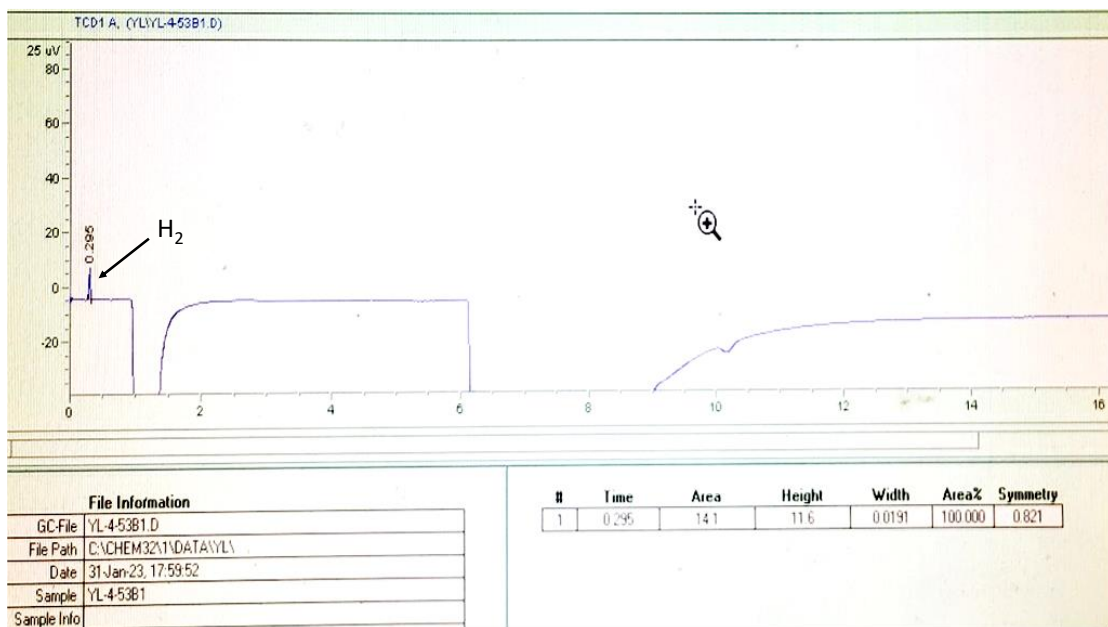


Figure S80. GC-TCD chromatogram of the gas phase above a solution of complex **5** as it transforms into complex **6**, which provided evidence for the evolution of dihydrogen gas (positive signal at 0.295 minutes).

5. X-ray data collection and structure refinement

Single crystals of the various complexes were obtained by dissolving each complex in an appropriate solvent, overlaying the solution with pentane, and storing the sample at room temperature under an N₂ atmosphere. In this manner, complex **2** was crystallized from CH₂Cl₂, **3** and **8** from THF, and **10-13** from acetone. All crystals were immersed in oil and flash-frozen in a liquid nitrogen stream before data collection, which was carried out at 100 K. Diffraction data for structures **2**, **3**, **10**, **11** and **13** were collected on a Rigaku Synergy-R diffractometer equipped with a HyPix ARC 150° detector, using CuK α radiation ($\lambda=1.54184\text{\AA}$). Diffraction data for structures **8** and **12** were collected on a Rigaku Synergy-S diffractometer dual source equipped with a Dectris Pilatus3 R CdTe 300K detector, using MoK α radiation ($\lambda=0.71073\text{\AA}$). Data were processed with CrysAlisPRO and structures were solved with SHELXT. [1] All non-hydrogen atoms were further refined by SHELXL [2] with anisotropic displacement coefficients. Hydrides were located in the electron density map. All other hydrogen atoms were placed in calculated positions and refined in a riding mode. Refinement was carried out with the OLEX-2 GUI. [3] The structure of complex **8** was refined as a twin, with a Flack parameter of 0.46. In the structure of complex **12**, two disordered molecules of acetone were omitted using the SQUEEZE procedure. [4]

Table S1. Crystallographic data for complexes **2**, **3**, **8** and **10-13**.

Species	Complex 2	Complex 3	Complex 8	Complex 10	Complex 11	Complex 12	Complex 13
CCDC No.	2224306	2243894	2243893	2224305	2224308	2224307	2224309
Formula*	C ₄₁ H ₃₅ ClIrNP ₂	2C ₂₇ H ₄₁ ClIrNP ₂ +0.67H ₂ O	C ₅₄ H ₈₄ Ir ₂ N _{3.6} P ₄	C ₇₈ H ₆₈ Ir ₂ N ₂ P ₄ +2C ₄ H ₈ O	2C ₄₇ H ₄₅ IrNP ₂ +2BF ₄ +3C ₃ H ₆ O	C ₄₇ H ₄₇ IrNP ₂ +BF ₄ +C ₃ H ₆ O	C ₄₇ H ₄₃ IrNP ₂ +BF ₄
Molecular weight*	831.29	1350.40	1291.36	1685.83	1080.94	1991.68	962.77
Crystal system	Monoclinic	Tetragonal	Triclinic	Monoclinic	Triclinic	Triclinic	Monoclinic
Space group	P ₂ / <i>n</i>	R̄3	P1	P ₂ / <i>n</i>	P̄1	P̄1	P ₂ / <i>c</i>
Crystal size (mm)	0.136×0.085×0.014	0.621×0.151×0.030	0.150×0.080×0.030	0.098×0.075×0.016	0.175×0.068×0.057	0.669×0.094×0.061	0.20×0.15×0.03
Crystal color and shape	Red plate	Orange Chunk	Orange Chunk	Light blue plate	Yellow needle	Yellow needle	Red plate
Temperature (K)	100	100	100	100	100	100	100
Wavelength (Å)	1.54184	1.54184	0.71073	1.54184	1.54184	0.71073	1.54184
<i>a</i> (Å)	10.2353(2)	23.8300(5)	11.1317(9)	14.6878(4)	11.0926(3)	11.1917(3)	11.1021(2)
<i>b</i> (Å)	15.7500(3)	23.8300(5)	11.3506(9)	15.8409(3)	14.0454(4)	13.9037(3)	16.4585(2)
<i>c</i> (Å)	20.1431(4)	25.9918(8)	12.1293(6)	15.3290(4)	16.9368(5)	16.9855(5)	21.5943(4)
α (°)	90	90	62.825(7)	90	72.748(3)	72.304(3)	90
β (°)	92.315(2)	90	73.192(6)	98.998(2)	74.351(3)	74.728(3)	102.532(2)
γ (°)	90	120	87.208(6)	90	87.175(2)	87.301(2)	90
Volume (Å ³)	3244.54(11)	12782.5(7)	1298.87(18)	3522.68(15)	2425.27(13)	2427.49(12)	3851.79(11)
<i>Z</i>	4	9	1	2	2	1	4
r_{calcd} (g·cm ⁻³)	1.702	1.579	1.651	1.589	1.480	1.362	1.66
μ (mm ⁻¹)	9.897	11.143	5.28	8.463	6.414	2.864	7.957
No. of reflections (unique)	74986 (6587)	63380 (5031)	19886 (8403)	80524 (7191)	46812 (8866)	49018 (8891)	51653 (7844)
R_{int}	0.0403	0.0712	0.0722	0.0464	0.0612	0.0461	0.0727
Completeness to θ (%)	99.3	100	91.8	99.8	99.9	100.0	99.5
θ max	74.489	66.599	25.022	74.492	68.247	25.347	74.494
Data / restraints / parameters	6587 / 0 / 415	5031 / 0 / 313	8403 / 487 / 559	7191 / 0 / 441	8866 / 438 / 737	8891 / 160 / 610	7844 / 0 / 505
Goodness-of-fit on F^2	1.037	1.025	1.076	1.072	1.058	1.062	1.000
Final R_1 and wR_2 indices [$I > 2s(I)$]	0.0315, 0.0796	0.0371, 0.0996	0.0794, 0.1676	0.0372, 0.0998	0.0485, 0.1299	0.0294, 0.0709	0.0390, 0.1033
R_1 and wR_2 indices (all data)	0.0379, 0.0840	0.0460, 0.1052	0.0969, 0.1764	0.0439, 0.1050	0.0604, 0.1360	0.0331, 0.0722	0.0449, 0.1069

6. Crystal structure of complex 8

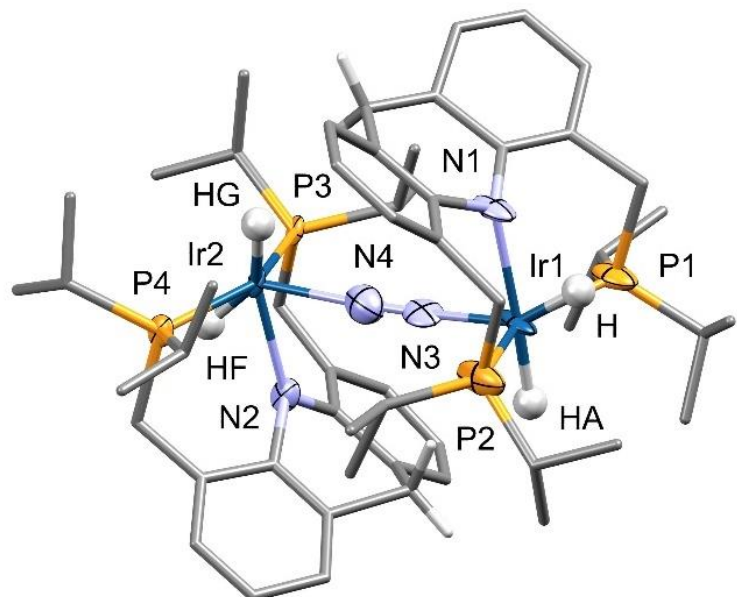


Figure S80. Crystal structure of complex **8**. Atoms belonging to the first coordination sphere are presented as thermal ellipsoids (50% probability), whereas the rest of the structure is represented by capped sticks. The iridium atoms are disordered and only those Ir atoms with largest site occupancy are shown. All H atoms were omitted for clarity, except for the hydride ligands and H atoms at the C9 position of each acridanide ligand. The hydrides were located in the electron density map and are presented as spheres. Atoms are color coded as follows: Ir, blue; N, light blue; C, gray; P, orange; H, white. Select distances (\AA) and angles ($^{\circ}$): P2–Ir1, 2.32(1); P1–Ir1, 2.29(1); N1–Ir1, 2.18(3); N3–Ir1, 1.99(4); N3–N4, 1.14(4); Ir2–N4, 2.14(4); P4–Ir2, 2.30(1); P3–Ir2, 2.299(8); N2–Ir2, 2.17(3); P4–Ir2–P3, 150.1(3), P4–Ir2–N2, 92(1); P3–Ir2–N4, 100.6(12); N2–Ir2–N4, 77(1); P1–Ir1–N1, 91(1); P1–Ir1–P2, 147.9(5); P1–Ir1–N1, 91(1); N1–Ir1–N3, 88(1).

7. ICP-OES measurements associated with complexes **5** and **9**

Solid precipitates were isolated during the syntheses of complexes **5** and **9** from precursors **3** and **4**, respectively. Samples from each precipitate were predigested in a mixture of HNO₃, HCl and H₂O₂, heated to a nominal temperature of 120 °C. The resulting mixture was subjected to ICP-OES analysis. Samples of complex **9** could not be fully dissolved, and the results are therefore qualitative. Iridium, sodium, phosphorus and boron were detected in both samples, and their concentrations are provided in the following table:

Element	Concentration (wt%)	
	Complex 5	Complex 9
B	0.15(2)	0.048(3)
Ir	12(1)	6.3(4)
Na	7(2)	3.1(1)
P	3.1(3)	1.59(9)

8. References

- [1] G.M. Sheldrick, *SHELXT – Integrated space-group and crystal-structure determination*, Acta Cryst. A71 (2015) 3–8.
<https://doi.org/10.1107/S2053273314026370>.
- [2] G.M. Sheldrick, A short history of *SHELX*, Acta Cryst. A64 (2008) 112–122.
<https://doi.org/10.1107/S0108767307043930>.
- [3] O. V. Dolomanov, L.J. Bourhis, R.J. Gildea, J.A.K. Howard, H. Puschmann, *OLEX2 : a complete structure solution, refinement and analysis program*, J. App. Cryst. 42 (2009) 339–341. <https://doi.org/10.1107/S0021889808042726>.
- [4] A. L. Spek: PLATON SQUEEZE: a tool for the calculation of the disordered solvent contribution to the calculated structure factors, Acta Cryst. C71 (2015) 9-18. <https://doi.org/10.1107/S2053229614024929>